RADC-TR-76-264
Interim Technical Report No. 12
August 1976

TRANSMISSION FROM A RECTANGULAR WAVEGUIDE INTO HALF SPACE THROUGH A RECTANGULAR APERTURE

Department of Electrical and Computer Engineering
Syracuse University

ROME AIR DEVELOPMENT CENTER
AIR FORCE SYSTEMS COMMAND
GRIFFISS AIR FORCE BASE, NEW YORK 13441

Professor Roger F. Harrington and Dr. J. R. Mautz are the co-responsible investigators for this contract. Peter R. Franchi (ETER) is the RADC Project Engineer.

This report has been reviewed by the RADC Information Office (OI) and is releasable to the National Technical Information Service (NTIS). At NTIS it will be releasable to the General public, including foreign nations.

This technical report has been reviewed and approved for publication.

APPROVED:

Peter R. Franchi

PETER R. FRANCHI
Project Engineer

APPROVED: Allan C. Schell

ALLAN C. SCHELL
Acting Chief
Electromagnetic Sciences Division

FOR THE COMMANDER: John P. Huss

Plans Office

UNCLASSIFIED

SECURITY CLASSIFICATION OF THIS PAGE (When Data Entered)

(19) REPORT DOCUMENTATION PAGE

READ INSTRUCTIONS BEFORE COMPLETING FORM

1. REPORT NUMBER (18) RADC-TR-76-264 ✓	2. GOVT ACCESSION NO.	3. RECIPIENT'S CATALOG NUMBER
4. TITLE (and Subtitle) (6) TRANSMISSION FROM A RECTANGULAR WAVEGUIDE INTO HALF SPACE THROUGH A RECTANGULAR APERTURE		5. TYPE OF REPORT & PERIOD COVERED (14) Scientific Report No. 12
		6. PERFORMING ORG. REPORT NUMBER
7. AUTHOR(s) (10) Joseph R./Mautz, Roger F./Harrington		8. CONTRACT OR GRANT NUMBER(s) (15) F19628-..-C-0047
9. PERFORMING ORGANIZATION NAME AND ADDRESS Syracuse University, Department of Electrical and Computer Engineering, Syracuse, New York 13210		10. PROGRAM ELEMENT, PROJECT, TASK AREA & WORK UNIT NUMBERS 5635-06-01
11. CONTROLLING OFFICE NAME AND ADDRESS Deputy of Electronic Technology (RADC), Hanscom AFB, Massachusetts 01731, Contract Monitor: Peter R. Franchi/ETER		12. REPORT DATE (11) August 1976
		13. NUMBER OF PAGES 55
14. MONITORING AGENCY NAME & ADDRESS(if different from Controlling Office) (9) Interim technical rept.,		15. SECURITY CLASS. (of this report) UNCLASSIFIED
		15a. DECLASSIFICATION/DOWNGRADING SCHEDULE

16. DISTRIBUTION STATEMENT (of this Report)

A - Approved for public release; distribution unlimited.

(12) 56p. (16) AF-5635 (17) 563506

17. DISTRIBUTION STATEMENT (of the abstract entered in Block 20, if different from Report)

18. SUPPLEMENTARY NOTES

19. KEY WORDS (Continue on reverse side if necessary and identify by block number)

Aperture admittance	Method of moments
Apertures in ground planes	Rectangular apertures
Computer program	Rectangular waveguides
Conducting plane	Waveguide-fed aperture

20. ABSTRACT (Continue on reverse side if necessary and identify by block number)

A computer program is developed for the problem of transmission of electromagnetic waves from a rectangular waveguide into half space through a rectangular aperture. The aperture may cover all or part of the waveguide cross section, but the sides of the aperture are parallel to those of the waveguide cross section. The solution uses the moment method applied to the integral equation for the equivalent magnetic current in the aperture. The expansion and testing functions are triangles in the direction of current, and pulses over

DD FORM 1473 1 JAN 73 EDITION OF 1 NOV 65 IS OBSOLETE

S/N 0102-014-6601

UNCLASSIFIED

SECURITY CLASSIFICATION OF THIS PAGE (When Data Entered)

406737 LB

transverse to the direction of current. Quantities computed are the equivalent magnetic current, the reflection coefficient and equivalent aperture admittance seen by the incident mode, and the radiation gain pattern. The computer program is described and listed with sample input-output data.

CONTENTS

Part One

Part Two

PART ONE

THEORY AND EXAMPLES

I. STATEMENT OF THE PROBLEM

Figure 1 shows the problem to be considered and defines the coordinates and parameters to be used. The perfectly conducting plate covers the entire $z=0$ plane except for the aperture which is rectangular in shape with side lengths $L_x \Delta x$ and $L_y \Delta y$ in the x and y directions respectively. L_x and L_y are positive integers and $L_x \geq 2$. The aperture is fed by a rectangular waveguide. The excitation of the waveguide is a source which produces one mode, of unit amplitude, which travels toward the aperture.

The general method of solution [1] is to cover the aperture with a perfect electric conductor, to place magnetic current sheets $+\underset{\sim}{M}$ and $-\underset{\sim}{M}$ respectively on the left-hand and right-hand sides of this conductor, to obtain an integral equation for $\underset{\sim}{M}$ by equating the tangential magnetic fields on both sides of this conductor, and to solve this integral equation using the method of moments. The testing functions are the same as the expansion functions for $\underset{\sim}{M}$ and are denoted by $\underset{\sim}{M}_i$. Each $\underset{\sim}{M}_i$ is a triangle in the direction of current flow and a pulse in the direction perpendicular to current flow.

II. SUMMARY OF BASIC THEORY

The solution for $\underset{\sim}{M}$ is given [1] by

$$\underset{\sim}{M} = \sum_i V_i \underset{\sim}{M}_i \tag{1}$$

where the V_i are elements of a column vector $\vec{V}$ given by

$$\vec{V} = [Y^{wg} + Y^{hs}]^{-1} \vec{I}^i . \tag{2}$$

Here,

$$Y_{ij}^{hs} = - \iint_{\text{apert.}} \underset{\sim}{M}_i \cdot \underset{\sim}{H}^{hs}(\underset{\sim}{M}_j)\, ds \tag{3}$$

[1] R. F. Harrington and J. R. Mautz, "A Generalized Network Formulation for Aperture Problems," Scientific Report No. 8 on Contract F19628-73-C-0047 with A. F. Cambridge Research Laboratories, Report AFCRL-TR-75-0589, November 1975.

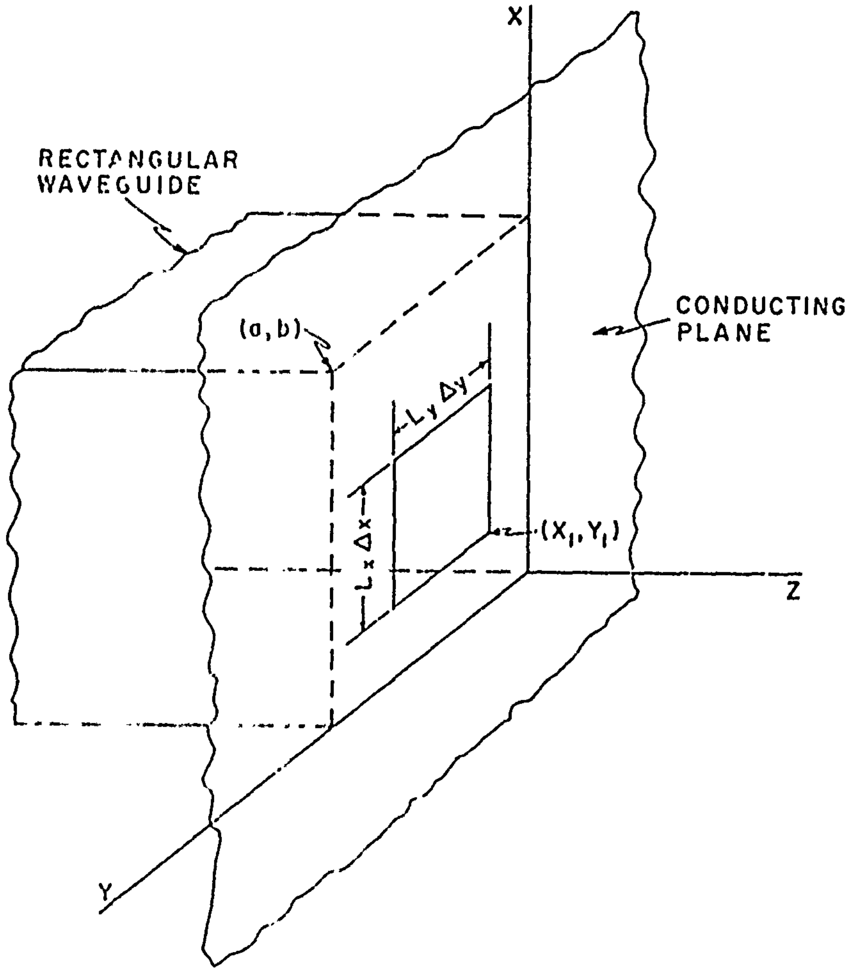

Fig. 1. A rectangular waveguide radiating through a rectangular aperture into half space bounded by an electric conductor.

where $\underset{\sim}{H}^{hs}(\underset{\sim}{M}_j)$ is the magnetic field at $z=0^+$ radiated by the magnetic current $\underset{\sim}{M}_j$ in front of the perfect electric conductor. Also,

$$Y_{ij}^{wg} = \sum_n A_{in} Y_n A_{jn} \tag{4}$$

and

$$I_j^i = 2Y_0 A_{j0} \tag{5}$$

where

$$A_{ij} = \iint_{\text{apert.}} \underset{\sim}{M}_i \cdot \underset{\sim}{u}_z \times \underset{\sim}{e}_j \, ds . \tag{6}$$

Here, $\underset{\sim}{u}_z$ is a unit vector in the z direction, $\underset{\sim}{e}_j$ is the jth waveguide mode, and Y_j is its characteristic admittance. The excited mode is $\underset{\sim}{e}_0$.

The coefficients Γ_j of the reflected waveguide modes are given by

$$\begin{aligned} 1 + \Gamma_0 &= \sum_i A_{i0} V_i \\ \Gamma_j &= \sum_i A_{ij} V_i , \quad j \neq 0 . \end{aligned} \tag{7}$$

The gain associated with the $\underset{\sim}{u}_m$ component of the magnetic field in the half-space $z > 0$ is given by

$$G = \frac{k^2}{8\pi\eta \, \mathrm{Re}(\vec{V}[Y^{hs}]^* \vec{V}^*)} |\tilde{P}^m \vec{V}|^2 \tag{8}$$

where η is the characteristic impedance of free space and

$$P_j^m = -2 \iint_{\text{apert.}} \underset{\sim}{M}_j \cdot \underset{\sim}{u}_m e^{-j\underset{\sim}{k}_m \cdot \underset{\sim}{r}} ds . \tag{9}$$

In (9), $\underset{\sim}{k}_m$ points from the distant observation point to the aperture and $|\underset{\sim}{k}_m|$ is the propagation constant k.

$[Y^{hs}]$ is $\frac{1}{2}$ times the admittance matrix dealt with in [2]. $\vec{P}^m$ has

[2] J. R. Mautz and R. F. Harrington, "Electromagnetic Transmission Through a Rectangular Aperture in a Perfectly Conducting Plane," Scientific Report No. 10 on Contract F19628-73-C-0047 with A.F. Cambridge Research Laboratories, Report AFCRL-TR-76-0056, February 1976.

been calculated in [2] for the special case $x_1 = y_1 = 0$. x_1 and y_1 are defined in Fig. 1. From (9), we see that $x_1 \neq 0$, $y_1 \neq 0$ merely introduces the phase factor $e^{-jx_1(\underset{\sim}{k}_m \cdot \underset{\sim}{u}_x) - jy_1(\underset{\sim}{k}_m \cdot \underset{\sim}{u}_y)}$ which is subsequently masked by the magnitude operation in (8). Now that $[Y^{hs}]$ and $\vec{P}_m$ are disposed of, all that remains to carry out the calculations (1) to (9) are detailed formulas for A_{ij} and Y_j.

III. COEFFICIENTS A_{ij} AND CHARACTERISTIC ADMITTANCES Y_j

Expression (6) for A_{ij} requires a knowledge of the expansion functions $\underset{\sim}{M}_i$ and waveguide modes $\underset{\sim}{e}_j$.

The set $\underset{\sim}{M}_i$ of expansion functions is split into a set $\underset{\sim}{M}_i^x$ of x directed magnetic currents and a set $\underset{\sim}{M}_i^y$ of y directed magnetic currents defined by

$$\underset{\sim}{M}^x_{p+(q-1)(L_x-1)} = \underset{\sim}{u}_x \, T^x_p(x-x_1) \, P^y_q(y-y_1) \begin{cases} p=1,2,\ldots L_x-1 \\ q=1,2,\ldots L_y \end{cases} \tag{10}$$

$$\underset{\sim}{M}^y_{p+(q-1)L_x} = \underset{\sim}{u}_y \, T^y_q(y-y_1) \, P^x_p(x-x_1) \begin{cases} p=1,2,\ldots L_x \\ q=1,2,\ldots L_y-1 \end{cases} \tag{11}$$

where $T^x_p(x)$ and $T^y_q(y)$ are triangle functions defined by

$$T^x_p(x) = \begin{cases} \dfrac{x-(p-1)\Delta x}{\Delta x} & (p-1)\Delta x \le x \le p\Delta x \\ \dfrac{(p+1)\Delta x - x}{\Delta x} & p\Delta x \le x \le (p+1)\Delta x \\ 0 & |x-p\Delta x| \ge \Delta x \end{cases} \tag{12}$$

$$T^y_q(y) = \begin{cases} \dfrac{y-(q-1)\Delta y}{\Delta y} & (q-1)\Delta y \le y \le q\Delta y \\ \dfrac{(q+1)\Delta y - y}{\Delta y} & q\Delta y \le y \le (q+1)\Delta y \\ 0 & |y-q\Delta y| \ge \Delta y \end{cases} \tag{13}$$

and $P^x_p(x)$ and $P^y_q(y)$ are pulse functions defined by

$$P_p^x(x) = \begin{cases} 1 & (p-1)\Delta x \leq x < p\Delta x \\ 0 & \text{all other } x \end{cases} \tag{14}$$

$$P_q^y(y) = \begin{cases} 1 & (q-1)\Delta y \leq y < q\Delta y \\ 0 & \text{all other } y \end{cases} \quad . \tag{15}$$

The set $\underset{\sim}{e}_j$ of modes for the rectangular waveguide is split into a set $\underset{\sim}{e}_j^{TE}$ of TE modes given by [3]

$$\underset{\sim}{e}^{TE}_{m+n(L_m+1)} = \sqrt{\frac{ab\ \varepsilon_m \varepsilon_n}{(mb)^2 + (na)^2}}\ [\underset{\sim}{u}_x \frac{n}{b} \cos \frac{m\pi x}{a} \sin \frac{n\pi y}{b} - \underset{\sim}{u}_y \frac{m}{a} \sin \frac{m\pi x}{a} \cos \frac{n\pi y}{b}] \tag{16}$$

$$m = 0,\ 1,2,\ldots L_m \qquad m + n \neq 0$$

$$n = 0,\ 1,2,\ldots L_n$$

$$\varepsilon_m = \begin{cases} 1 & m = 0 \\ 2 & m = 1,2,\ldots \end{cases}$$

and a set e_j^{TM} of TM modes given by

$$\underset{\sim}{e}^{TM}_{m+(n-1)L_m} = 2\sqrt{\frac{ab}{(mb)^2+(na)^2}}[\underset{\sim}{u}_x \frac{m}{a} \cos \frac{m\pi x}{a} \sin \frac{n\pi y}{b} + \underset{\sim}{u}_y \frac{n}{b} \sin \frac{m\pi x}{a} \cos \frac{n\pi y}{b}] \tag{17}$$

$$m = 1,2,3,\ldots L_m$$

$$n = 1,2,3,\ldots L_n \quad .$$

With the separation of $\underset{\sim}{M}_i$ into $\underset{\sim}{M}_i^x$ and $\underset{\sim}{M}_i^y$ and $\underset{\sim}{e}_j$ into $\underset{\sim}{e}_j^{TE}$ and $\underset{\sim}{e}_j^{TM}$, A_{ij} of (6) expands to

[3] R. F. Harrington, "Time-Harmonic Electromagnetic Fields," McGraw-Hill Book Company, New York, 1961, Equations (8-34), (3-86), and (3-89) and Section 4-3.

$$A_{ij}^{xTE} = \iint_{\text{apert.}} \underset{\sim}{M}_i^x \cdot \underset{\sim}{u}_z \times \underset{\sim}{e}_j^{TE} \, ds \tag{18}$$

$$A_{ij}^{yTE} = \iint_{\text{apert.}} \underset{\sim}{M}_i^y \cdot \underset{\sim}{u}_z \times \underset{\sim}{e}_j^{TE} \, ds \tag{19}$$

$$A_{ij}^{xTM} = \iint_{\text{apert.}} \underset{\sim}{M}_i^x \cdot \underset{\sim}{u}_z \times \underset{\sim}{e}_j^{TM} \, ds \tag{20}$$

$$A_{ij}^{yTM} = \iint_{\text{apert.}} \underset{\sim}{M}_i^y \cdot \underset{\sim}{u}_z \times \underset{\sim}{e}_j^{TM} \, ds \, . \tag{21}$$

Here, $\underset{\sim}{M}_i^x$, $\underset{\sim}{M}_i^y$, $\underset{\sim}{e}_j^{TE}$, and $\underset{\sim}{e}_j^{TM}$ are given by (10), (11), (16), and (17) respectively.

A tedious but straightforward evaluation of the integrals appearing in (18) to (21) leads to

$$\sqrt{\frac{2\pi}{\Delta x \Delta y}}\, A_{ij}^{xTE} = \sqrt{\frac{4\pi \Delta x \Delta y \varepsilon_n}{ab}} \left(\frac{m\pi}{k_j a}\right) \left(\frac{\sin\frac{m\pi\Delta x}{2a}}{\frac{m\pi\Delta x}{2a}}\right)^2 \left(\frac{\sin\frac{n\pi\Delta y}{2b}}{\frac{n\pi\Delta y}{2b}}\right)$$

$$\sin\frac{m\pi(x_1 + p\Delta x)}{a} \cos\frac{n\pi(y_1 + (q-1/2)\Delta y)}{b} \tag{22}$$

$$\sqrt{\frac{2\pi}{\Delta x \Delta y}}\, A_{ij}^{yTE} = \sqrt{\frac{4\pi \Delta x \Delta y \varepsilon_m}{ab}} \left(\frac{n\pi}{k_j b}\right) \left(\frac{\sin\frac{n\pi\Delta y}{2b}}{\frac{n\pi\Delta y}{2b}}\right)^2 \left(\frac{\sin\frac{m\pi\Delta x}{2a}}{\frac{m\pi\Delta x}{2a}}\right)$$

$$\cos\frac{m\pi(x_1 + (p-1/2)\Delta x)}{a} \sin\frac{n\pi(y_1 + q\Delta y)}{b} \tag{23}$$

$$\sqrt{\frac{2\pi}{\Delta x \Delta y}}\, A_{ij}^{xTM} = -\sqrt{\frac{8\pi\Delta x\Delta y}{ab}}\, (\frac{n\pi}{k_j b}) \left(\frac{\sin\frac{m\pi\Delta x}{2a}}{\frac{m\pi\Delta x}{2a}}\right)^2 \left(\frac{\sin\frac{n\pi\Delta y}{2b}}{\frac{n\pi\Delta y}{2b}}\right)$$

$$\sin\frac{m\pi(x_1 + p\Delta x)}{a} \cos\frac{n\pi(y_1 + (q-1/2)\Delta y)}{b} \qquad (24)$$

$$\sqrt{\frac{2\pi}{\Delta x \Delta y}}\, A_{ij}^{yTM} = \sqrt{\frac{8\pi\Delta x\Delta y}{ab}}\, (\frac{m\pi}{k_j a}) \left(\frac{\sin\frac{n\pi\Delta y}{2b}}{\frac{n\pi\Delta y}{2b}}\right)^2 \left(\frac{\sin\frac{m\pi\Delta x}{2a}}{\frac{m\pi\Delta x}{2a}}\right)$$

$$\cos\frac{m\pi(x_1 + (p-1/2)\Delta x)}{a} \sin\frac{n\pi(y_1 + q\Delta y)}{b} \qquad (25)$$

where

$$k_j = \sqrt{(\frac{m\pi}{a})^2 + (\frac{n\pi}{b})^2}\ . \qquad (26)$$

In (22) and (24),

$$i = p + (q-1)(L_x-1) \quad \begin{cases} p = 1,2,\ldots L_x-1 \\ q = 1,2,\ldots L_y \end{cases} \qquad (27)$$

whereas in (23) and (25),

$$i = p + (q-1)L_x \quad \begin{cases} p = 1,2,\ldots L_x \\ q = 1,2,\ldots L_y-1 \end{cases} . \qquad (28)$$

In (22) and (23),

$$j = m + n\ (L_m+1) \quad \begin{cases} m = 0,1,2,\ldots L_m \\ n = 0,1,2,\ldots L_n \end{cases} m+n \neq 0 \qquad (29)$$

whereas in (24) and (25),

$$j = m + (n-1)L_m \quad \begin{cases} m = 1,2,\ldots L_m \\ n = 1,2,\ldots L_n \end{cases} . \qquad (30)$$

If m or n is zero in (22) or (23), the resulting $(\frac{\sin 0}{0})$ is to be replaced by unity.

The characteristic admittances Y_j of the rectangular waveguide with relative dielectric constant ε_r and relative permeability unity are classified as either TE admittances Y_j^{TE} or TM admittances Y_j^{TM} given by [3]

$$-j\eta Y_j^{TE} = \begin{cases} -\sqrt{(\frac{k_j}{k})^2 - \varepsilon_r} & k\sqrt{\varepsilon_r} < k_j \\ -j\sqrt{\varepsilon_r - (\frac{k_j}{k})^2} & k\sqrt{\varepsilon_r} > k_j \end{cases} \tag{31}$$

$$-j\eta Y_j^{TM} = \begin{cases} \dfrac{\varepsilon_r}{\sqrt{(\frac{k_j}{k})^2 - \varepsilon_r}} & k\sqrt{\varepsilon_r} < k_j \\ \dfrac{-j\varepsilon_r}{\sqrt{\varepsilon_r - (\frac{k_j}{k})^2}} & k\sqrt{\varepsilon_r} > k_j \ . \end{cases} \tag{32}$$

In (31) and (32), η is the characteristic impedance of free space, k is the free space wave number, and k_j is the cutoff wave number given by (26). Strictly speaking, we should have defined separate cutoff wave numbers, say k_j^{TE} and k_j^{TM}, for TE and TM modes because the relationship between j, m, and n in (26) is given by (29) for TE modes and by (30) for TM modes.

IV. POSSIBLE DIFFICULTY AT CUTOFF FREQUENCIES OF TM MODES

If $k_j = k\sqrt{\varepsilon_r}$, then Y_j^{TM} of (32) tends to infinity. Assume that k_j is very close to $k\sqrt{\varepsilon_r}$ for $j = j_1, j_2, j_3, \ldots j_L$ and rewrite $[Y^{wg} + Y^{hs}]$ of (2) as

$$[Y^{wg} + Y^{hs}] = [B\tilde{B} + C] \tag{33}$$

where

$$B_{i\ell} = \sqrt{Y^{TM}_{j_\ell}}\, A^{TM}_{ij_\ell}\ , \quad \ell = 1,2,3,\ldots L \tag{34}$$

$$C_{ij} = Y^{hs}_{ij} + \sum_n A^{TE}_{in}\, Y^{TE}_n\, A^{TE}_{jn} + \sum_n{}' \; A^{TM}_{in}\, Y^{TM}_n\, A^{TM}_{jn} \tag{35}$$

where $\sum_n{}'$ denotes the sum over all n except $n=j_1, j_2, j_3, \ldots j_L$. Also,

$$\begin{aligned} A^{TE}_{in} &= A^{xTE}_{in}\ , \quad i = 1,2,\ldots (L_x-1)L_y \\ A^{TE}_{i+(L_x-1)L_y,n} &= A^{yTE}_{in}\ , \quad i = 1,2,\ldots L_x(L_y-1) \end{aligned} \tag{36}$$

and A^{TM}_{in} is given by (36) with superscripts TE replaced by TM. The A^{xTE}_{in}, A^{yTE}_{in}, A^{xTM}_{in}, and A^{yTM}_{in} are defined by (18) to (21)

Substituting (33) into (2), we obtain

$$\vec{V} = [B\tilde{B} + C]^{-1}\, \vec{I}^{i} \tag{37}$$

Let

$$\vec{V} = B\vec{\alpha} + \vec{V}_2 \tag{38}$$

and choose $\vec{\alpha}$ such that

$$\tilde{B}\, \vec{V}_2 = 0 \tag{39}$$

Next, we substitute (38) into the form

$$\vec{I}^{i} = [B\tilde{B} + C]\vec{V} \tag{40}$$

of (37) and use (39) to obtain

$$\vec{I}^{i} = [B\tilde{B} + C]\, B\vec{\alpha} + C\vec{V}_2 \tag{41}$$

Expression (41) is premultiplied by C^{-1} resulting in

$$\vec{V}_2 = C^{-1}\vec{I}^{i} - [C^{-1}B\tilde{B} + U]\, B\vec{\alpha} \tag{42}$$

where U is the identity matrix. To obtain α, premultiply (42) by $\tilde{B}$ and use (39).

$$\vec{\alpha} = [\tilde{B}B]^{-1}[\tilde{B}C^{-1}B + U]^{-1}\tilde{B}C^{-1}\vec{I}^{i} \tag{43}$$

The solution for $\vec{V}$ is obtained by substituting (42) and (43) into (38).

$$\vec{V} = C^{-1}\vec{I}^{i} - C^{-1}B[\tilde{B}C^{-1}B + U]^{-1}\tilde{B}C^{-1}\vec{I}^{i} \tag{44}$$

When $Y^{TM}_{j_\ell}$, $\ell = 1,2,\ldots L$, tend to infinity, all the elements of B_{i_ℓ} also tend to infinity. Hence we are justified in substituting the approximation

$$[\tilde{B}C^{-1}B + U]^{-1} \approx [\tilde{B}C^{-1}B]^{-1} - [\tilde{B}C^{-1}B]^{-2} + [\tilde{B}C^{-1}B]^{-3} \tag{45}$$

where the superscripts -2 and -3 denote respectively the square and cube of the inverse matrix, into (44) with the result

$$\vec{V} = C^{-1}\vec{I}^{i} - C^{-1}B[\tilde{B}C^{-1}B]^{-1}\tilde{B}C^{-1}\vec{I}^{i} + C^{-1}B[\tilde{B}C^{-1}B]^{-2}\tilde{B}C^{-1}\vec{I}^{i} - C^{-1}B[\tilde{B}C^{-1}B]^{-3}\tilde{B}C^{-1}\vec{I}^{i}. \tag{46}$$

Consider the case in which the waveguide excitation is neither the j_1th nor the j_2th... nor the j_Lth TM mode. As $Y^{TM}_{j_\ell}$, $\ell = 1,2,\ldots L$ approach infinity, (46) approaches

$$\vec{V} = C^{-1}\vec{I}^{i} - C^{-1}D[\tilde{D}C^{-1}D]^{-1}\tilde{D}C^{-1}\vec{I}^{i} \tag{47}$$

where

$$D_{i\ell} = A^{TM}_{ij_\ell}\ , \quad \ell = 1,2,3,\ldots L \tag{48}$$

Substitution of (47) into (7) gives Γ^{TE}_{j} for all j and Γ^{TM}_{j} for all j except $j = j_1, j_2 \cdots j_L$. Here, Γ^{TE}_{j} is the coefficient of the jth TE reflected mode and Γ^{TM}_{j} is the coefficient of the jth TM reflected mode. Expression (47) gives $\Gamma^{TM}_{j_\ell} = 0, \ell = 1,2,\ldots L$. To investigate the manner in which $\Gamma^{TM}_{j_\ell}$ approaches zero, retain one more term in (46).

$$\vec{V} = C^{-1}\vec{I}^{i} - C^{-1}B[\tilde{B}C^{-1}B]^{-1}\tilde{B}C^{-1}\vec{I}^{i} + C^{-1}B[\tilde{B}C^{-1}B]^{-2}\tilde{B}C^{-1}\vec{I}^{i} \tag{49}$$

Premultiplying (49) by $\tilde{B}$, we obtain

$$\tilde{B}\vec{V} = [\tilde{B}C^{-1}B]^{-1}\tilde{B}C^{-1}\vec{I}^{i} \tag{50}$$

which, in view of (7), (34), and (48), leads to

$$Y_{j_\ell}^{TM}\,\Gamma_{j_\ell}^{TM} = ([\tilde{D}C^{-1}D]^{-1}\tilde{D}C^{-1}\vec{I}^{i})_\ell \tag{51}$$

where $(\ )_\ell$ denotes the ℓth element of the column vector inside the parentheses. From (51) we conclude that, for the case in which the waveguide excitation is neither the j_1th nor the j_2th ... nor the j_Lth TM mode, as $Y_{j_\ell}^{TM}, \ell = 1,2,\ldots L$ approach infinity the magnetic field of the j_ℓth, $\ell = 1,2,\ldots L$ TM mode approaches a finite limit and the complex power associated with this mode approaches zero.

Next, consider the case in which the waveguide excitation is the j_pth, $1 \le p \le L$, TM mode. From (5) and (48), $\vec{I}^{i}$ is $2Y_{j_p}^{TM}$ times the pth column of D. The column vector consisting of the first two terms in (46) is zero because it is $2Y_{j_p}^{TM}$ times the pth column of the matrix

$$C^{-1}D - C^{-1}D[\tilde{D}C^{-1}D]^{-1}\tilde{D}C^{-1}D$$

all of whose elements are precisely zero. Hence for large $Y_{j_\ell}^{TM}$, $\ell = 1,2,\ldots L$, (46) becomes

$$\vec{V} = C^{-1}B[\tilde{B}C^{-1}B]^{-2}\tilde{B}C^{-1}\vec{I}^{i} \tag{52}$$

which reduces to

$$\vec{V} = 2(C^{-1}D[\tilde{D}C^{-1}D]^{-1})_p \tag{53}$$

where $(\ )_p$ denotes the pth column vector of the matrix inside the parentheses. Expression (53) gives $\Gamma_{j_p}^{TM} = 1$ and $\Gamma_{j_\ell}^{TM} = 0$, $\ell \neq p$. By retaining the last term in (46) we obtain the more accurate representations

$$\Gamma^{TM}_{j_p} = 1 - \frac{\beta_{pp}}{Y^{TM}_{j_p}} \tag{54}$$

$$\Gamma^{TM}_{j_\ell} = - \frac{\beta_{\ell p}}{Y^{TM}_{j_\ell}} , \quad \ell \neq p \tag{55}$$

where

$$\beta_{\ell p} = 2 \, ([\tilde{D}C^{-1}D]^{-1})_{\ell p} \; . \tag{56}$$

Here, $(\ )_{\ell p}$ denotes the ℓpth element of the matrix inside the parentheses. From (54) and (55), we conclude that, for the case in which the waveguide excitation is the j_pth TM mode, as $Y^{TM}_{j_\ell}$, $\ell = 1,2,\ldots L$ approach infinity the aperture electric field due to the j_1th, j_2th ... j_Lth TM modes approaches twice the electric field of the incident mode and the aperture magnetic field due to these modes approaches a finite limit. The complex power associated with the j_pth TM waveguide mode approaches $2\beta^*_{pp}$ and that associated with the j_ℓth, $\ell \neq p$ TM waveguide mode approaches zero. The following line of reasoning shows that Real $(\beta_{pp}) > 0$. From power considerations $[C + C^*]$ is positive definite. Hence $[C^{-1} + [C^{-1}]^*]$, $[\tilde{D}C^{-1}D + [\tilde{D}C^{-1}D]^*]$, and $[[\tilde{D}C^{-1}D]^{-1} + [[\tilde{D}C^{-1}D]^{-1}]^*]$ are in turn positive definite and finally Real $(\beta_{pp}) > 0$.

We did not incorporate any of the logic (33) to (56) into the computer program because we contend that the simple precaution of replacing $(\frac{k_j}{k})^2 - \varepsilon_r$ of (31) and (32) by $10^{-6}\varepsilon_r$ whenever the calculated value of $(\frac{k_j}{k})^2 - \varepsilon_r$ is zero is adequate. Denoting $(\frac{k_j}{k})^2 - \varepsilon_r$ by δ_j, we justify this contention as follows. For seven decimal digit accuracy, the calculated value of $|\delta_j|$ must be exactly zero or be of the order $10^{-6}\varepsilon_r$ or larger. Hence, we assume that $|\delta_j|$ is roughly $10^{-6}\varepsilon_r$ or larger. In the following numerical investigation, what appears to be a reasonably accurate solution for $\vec{V}$ was obtained for $|\delta_j|$ in the neighborhood of $10^{-6}\varepsilon_r$. We set

$$L_x = L_y = L_m = L_n = 4, \quad \Delta x = \Delta y = \frac{\lambda}{4\sqrt{2}}, \quad a = b = \frac{\lambda}{\sqrt{2}}, \; x_1 = y_1 = 0$$

and $\varepsilon_r = 1$ such that $\delta_j \to 0$ for the TM_{11} mode. Successively, we let

$$\delta_j = -2.38 \times 10^{-7}, -2.5 \times 10^{-5}, -10^{-6}, 10^{-6}, -10^{-12}, -10^{-18}.$$

The first value -2.38×10^{-7} was the spontaneously calculated value of δ_j. When the waveguide excitation was the dominant TE mode, the elements of the computed solution $\vec{V}$ for the first four values of δ_j agreed to within a fraction of a percent of the magnitude of the largest element of $\vec{V}$. In going to $\delta_j = -10^{-12}$, the elements of $\vec{V}$ changed by only a few percent whereas for $\delta_j = -10^{-18}$, the computed solution $\vec{V}$ was absurdly inaccurate. When the waveguide excitation was the TM_{11} mode, the first four values of δ_j gave solutions $\vec{V}$ differing by less than one percent whereas the computed solutions $\vec{V}$ for the last two values -10^{-12} and -10^{-18} were absurdly inaccurate.

V. SYMMETRY OF THE ADMITTANCE MATRIX

The admittance matrix

$$Y = [Y^{wg} + Y^{hs}]$$

appearing in (2) will be shown to be symmetric.

From (4), Y^{wg} is symmetric.

Y^{hs} is $\frac{1}{2}$ times the admittance matrix dealt with in [2]. One might argue that Y^{hs} is symmetric because of the fact that the set of testing functions is the same as the set of expansion functions and because of reciprocity. However, this argument is not strictly correct because in [2] the integrations over source and field regions are approximated differently. Nevertheless, the matrix $2Y^{hs}$ given by [2, Eqs. (23) to (26)] is symmetric because one can show that

$$Y_{ij}^{xx} = Y_{ji}^{xx}$$

$$Y_{ij}^{yx} = Y_{ji}^{xy}$$

$$Y_{ij}^{yy} = Y_{ji}^{yy}$$

The symmetry of Y^{hs} is not due to reciprocity but due to the fact that of two rectangular subareas, the first as seen from the second is the same as the second as seen from the first.

VI. CONTINUITY OF COMPLEX POWER FLOW

It will be shown that the complex power flow associated with the method of moments solution (2) is continuous across the aperture.

From (2),

$$\vec{I}^{i} = [Y^{wg} + Y^{hs}]\vec{V} \tag{57}$$

Premultiplying the complex conjugate of (57) by $\tilde{V}$, we obtain

$$\tilde{V}\vec{I}^{i*} = \tilde{V}[Y^{wg*} + Y^{hs*}]\vec{V}^{*} \tag{58}$$

which is the same as

$$\tilde{V}\vec{I}^{i*} - \tilde{V}Y^{wg*}\vec{V}^{*} = \tilde{V}Y^{hs*}\vec{V}^{*} . \tag{59}$$

From [1, Eq. (27)], the right-hand side of (59) is the complex power radiated into half space. A development similar to that of [1, Eqs. (22) to (27)] shows that the left-hand side of (59) is the complex power flowing out of the waveguide. In (59), $\tilde{V}\vec{I}^{i*}$ represents the interaction of the magnetic current with the incident magnetic field whereas $\tilde{V}Y^{wg*}\vec{V}^{*}$ represents the interaction of the magnetic current with the magnetic field due to the magnetic current.

The above demonstration of continuity of complex power flow is based on the assumption that Y^{hs} is given by (3) and that Y^{wg} is given by (4). In reality, the integration (3) is approximated in [2] and only a finite number of terms of the infinite sum (4) are retained. As a result, (59) is still true but the right and left-hand sides of (59) are merely approximations to the complex power flow on both sides of the aperture. This is tolerable because the obvious way to obtain more accurate complex powers would be to calculate Y^{wg} and Y^{hs} more accurately. Now, these more accurate Y^{wg} and Y^{hs} should have been used in the method of moments solution and if they were used then the right and left-hand sides of (59) would be more accurate approximations to the complex power flow on both sides of the aperture.

Since the left-hand side of (59), henceforth denoted by P_{wg}

$$P_{wg} = \tilde{V}\vec{I}^{i*} - \tilde{V}Y^{wg*}\vec{V}^{*} \tag{60}$$

is the complex power flow on the waveguide side of the aperture, P_{wg} should be expressible solely in terms of the coefficients Γ_j of the reflected waveguide modes and the characteristic admittances Y_j. Substituting (4) and (5) into (60), we obtain

$$P_{wg} = 2Y_0^{*} \sum_j A_{j0}V_j - \sum_n Y_n^{*} \left(\sum_i A_{in}V_i\right) \left(\sum_j A_{jn}V_j^{*}\right) . \tag{61}$$

With the help of (7), (61) becomes

$$P_{wg} = Y_0^{*}(1 + \Gamma_0)\ (1 - \Gamma_0^{*}) - \sum_{n\neq 0} Y_n^{*}|\Gamma_n|^2 \tag{62}$$

which, in view of [1, Eqs. (22), (45), and (48)], is not surprising.

VII. NUMBER OF WAVEGUIDE MODES REQUIRED

The nth term in (4) represents the contribution of the nth waveguide mode to Y^{wg}. The contributions of the TE_{mn} and TM_{mn} waveguide modes are governed by the $(\frac{\sin x}{x})$ type factors appearing in (22) to (25). Hence, these contributions begin to fade away gradually as soon as

$$\frac{m\Delta x}{2a} > 1$$

$$\frac{n\Delta y}{2b} > 1 \cdot$$

From (44), (34), and (7), it is evident that if a solution V gives

$$\Gamma_j = 0 , \quad j \neq 0$$

$$\text{or} \qquad 1 + \Gamma_j = 0 , \; j = 0$$

then the jth term in (4) has no influence on $\vec{V}$ and therefore may be neglected.

If the aperture is centered about x = a/2 or y = b/2 or both, then it will be shown that several of the Γ_j are zero. The operator equation [1, Eq. (4)]

$$\underset{\sim}{H}_t^a(\underset{\sim}{M}) + \underset{\sim}{H}_t^b(\underset{\sim}{M}) = - \underset{\sim}{H}_t^i \tag{63}$$

preserves certain symmetry properties of the transverse component $\underset{\sim}{H}_t^i$ of the incident magnetic field. For instance, if the aperture is centered about x = a/2 and if $\underset{\sim}{H}_t^i$ has one of the symmetry properties

1) x component even about x = a/2, y component odd about x = a/2
2) x component odd about x = a/2, y component even about x = a/2

then the magnetic current $\underset{\sim}{M}$ has the same symmetry property. Also, if the aperture is centered about y = b/2 and if $\underset{\sim}{H}_t^i$ has one of the symmetry properties

3) x component even about y = b/2, y component odd about y = b/2
4) x component odd about y = b/2, y component even about y = b/2

then $\underset{\sim}{M}$ has the same symmetry property. The above symmetry relations between $\underset{\sim}{M}$ and $\underset{\sim}{H}_t^i$ will be verified later on in this section. It follows that if the aperture is centered about x = a/2 and if $\underset{\sim}{H}_t^i$ has symmetry property 1) then $\Gamma_j = 0$ for all modes which have symmetry property 2) whereas if $\underset{\sim}{H}_t^i$ has symmetry property 2) then $\Gamma_j = 0$ for all modes which have symmetry property 1). Likewise, if the aperture is centered about y = b/2 then $\Gamma_j = 0$ for all modes which have either symmetry property 4) or 3) depending on whether $\underset{\sim}{H}_t^i$ has symmetry property 3) or 4). Moreover, because $\underset{\sim}{H}_t^i$ is the transverse magnetic field of one of the waveguide modes defined by [1, Eq. (45)], (16), and (17), $\underset{\sim}{H}_t^i$ has either symmetry property 1) or 2) as well as either symmetry property 3) or 4).

The symmetry relations between $\underset{\sim}{M}$ and $\underset{\sim}{H}_t^i$ will now be verified. As far as symmetry properties 1), 2), 3), and 4) are concerned, $\underset{\sim}{H}_t^a(\underset{\sim}{M})$ has the same symmetry properties as $\underset{\sim}{M}$ because the operator $\underset{\sim}{H}_t^a$ merely alters the coefficients of the expansion of $\underset{\sim}{M}$ in terms of the transverse magnetic fields of the waveguide modes and can not introduce any new modes. From [2, Section III],

$$\underset{\sim}{H}^b(\underset{\sim}{M}) = -2j\omega\underset{\sim}{F} - 2\underset{\sim}{\nabla}\phi \tag{64}$$

where

$$\underset{\sim}{F} = \frac{\varepsilon}{4\pi} \iint_{\text{apert}} \underset{\sim}{M} \frac{e^{-jk|\underset{\sim}{r}-\underset{\sim}{r}'|}}{|\underset{\sim}{r}-\underset{\sim}{r}'|} ds \tag{65}$$

$$\phi = \frac{1}{4\pi\mu} \iint_{\text{apert.}} \rho \frac{e^{-jk|\underset{\sim}{r}-\underset{\sim}{r}'|}}{|\underset{\sim}{r}-\underset{\sim}{r}'|} \tag{66}$$

$$\rho = \frac{\underset{\sim}{\nabla}\cdot\underset{\sim}{M}}{-j\omega} \tag{67}$$

where $\underset{\sim}{r}$ and $\underset{\sim}{r}'$ are respectively the vectors to the field and source points in the aperture, ω is the angular frequency, ε is the capacitivity of free space, μ is the permeability of free space, and $k = \omega\sqrt{\mu\varepsilon}$ is the propagation constant in free space. We form a table of symmetry properties of ρ versus those of $\underset{\sim}{M}$.

SYMMETRY PROPERTY OF $\underset{\sim}{M}$	SYMMETRY PROPERTY OF ρ
1)	odd about $x = a/2$
2)	even about $x = a/2$
3)	even about $y = b/2$
4)	odd about $y = b/2$

If the aperture is centered about $x = a/2$ then ϕ of (66) is either even or odd about $x = a/2$ depending on whether ρ is even or odd about $x = a/2$. Similarly, if the aperture is centered about $y = b/2$ then ϕ is either even or odd about $y = b/2$ depending on whether ρ is even or odd about $y = b/2$. Hence ϕ has the same symmetry properties as ρ. Therefore, as regards symmetry properties 1), 2), 3), and 4), $\nabla\phi$ has the same symmetry properties as M. Since the x and y components of F are integrals of the same form as the integral which ϕ is, $F \cdot u_x$ has the same even or odd properties about x = a/2, y = b/2 as $M \cdot u_x$ while $F \cdot u_y$ has the same even or odd properties about x = a/2, y = b/2 as $M \cdot u_y$. Thus $H_t^a(M) + H_t^b(M)$ has the same symmetry properties as M. From this, it follows that M has the same symmetry properties as H_t^i.

VIII. SAMPLE COMPUTATIONS

A computer program using the formulas derived in the preceding sections has been written. It is described and listed in Part II of this report. In this section we give some examples of the computations that can be made using the general program.

Figure 2 shows the equivalent magnetic current for a rectangular waveguide of dimensions λ by $\lambda/2$ radiating into half space through a narrow centered rectangular slot of dimensions λ by $\lambda/10$. Figure 2(a) shows the x-component of equivalent magnetic current, which is also equal to the y-component of tangential E field in the slot. No y-component of magnetic current was obtained because only one pulse in y was used. M is normalized with respect to

$$\sqrt{\frac{1}{ab}\iint_{wg} |E^i|^2 \, dx\, dy} \tag{68}$$

where the integral is over the waveguide cross section. In other words, the normalization factor is the root-mean-square value of the incident E field. The phase of M is with respect to that of the incident electric field at the aperture. All computations are for dominant TE_{10} mode excitation. Figure 2(b) shows the radiation gain patterns in the two planes x = 0 and y = 0. The notation $G_{\theta y}$ denotes the gain pattern due to H_θ in the y = 0 plane. The notation G_{xx} denotes the gain pattern due to H_x in the x = 0 plane. The horizontal axis in Figure 2 is the z axis.

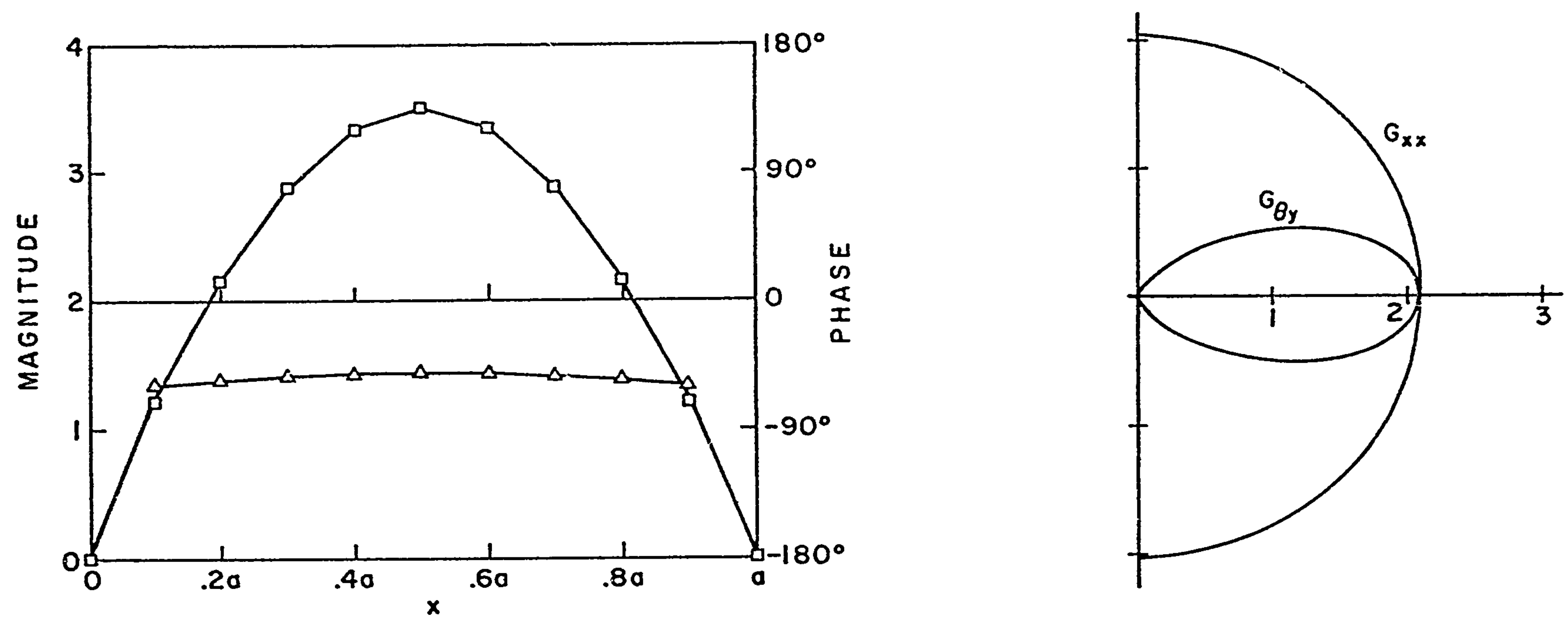

(a) Magnetic current

(b) Gain patterns

Fig. 2. Equivalent magnetic current M_x and radiation gain patterns for a rectangular waveguide of dimensions λ by λ/2 radiating through a centered rectangular slot of dimensions λ by λ/10. Squares denote magnitude and triangles denote phase.

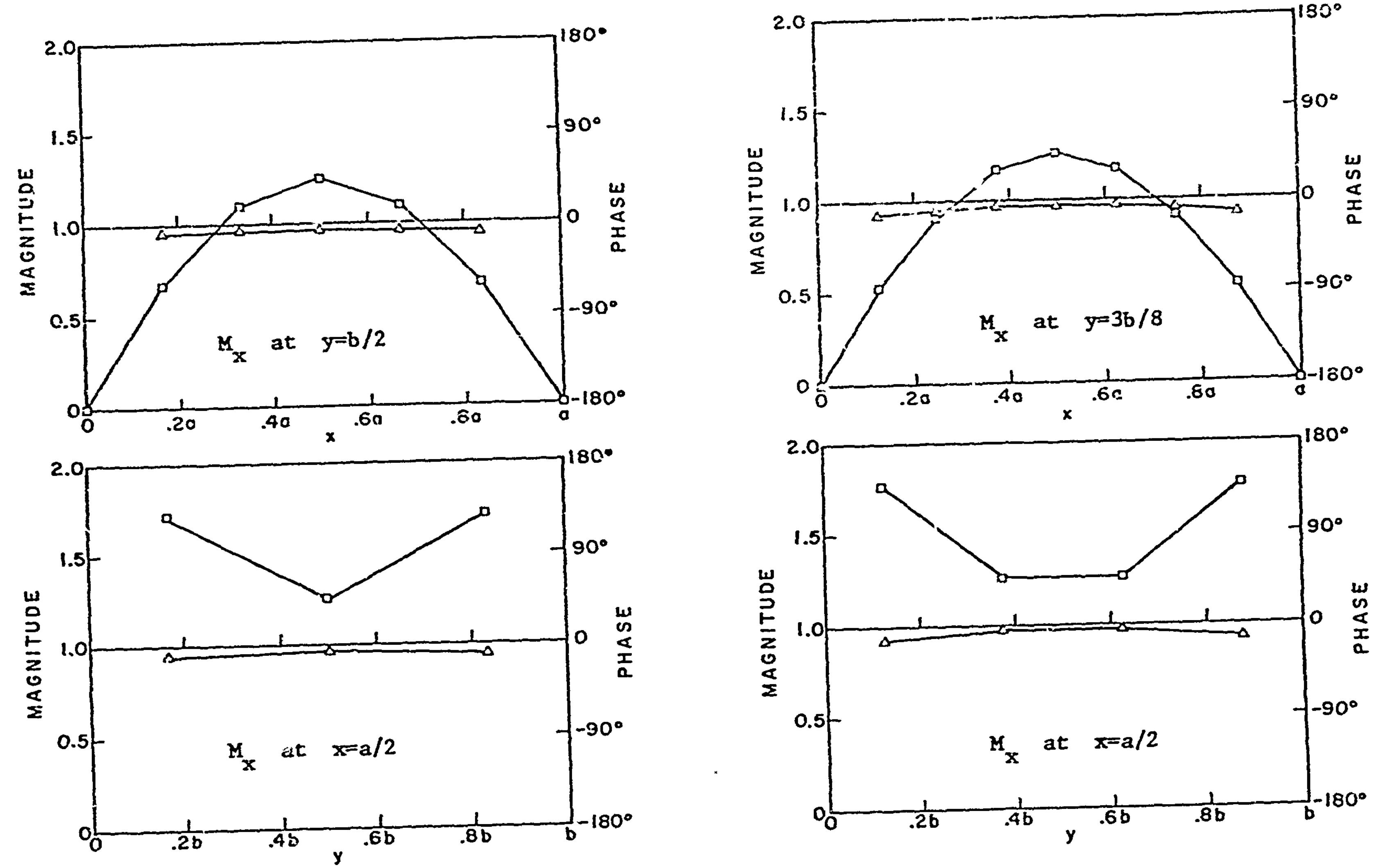

(a) a = 0.6λ

(b) a = 0.8λ

Fig. 3. Equivalent magnetic current for an open-ended rectangular waveguide of dimensions a/b = 2.25 radiating into half space. Squares denote magnitude, triangles denote phase.

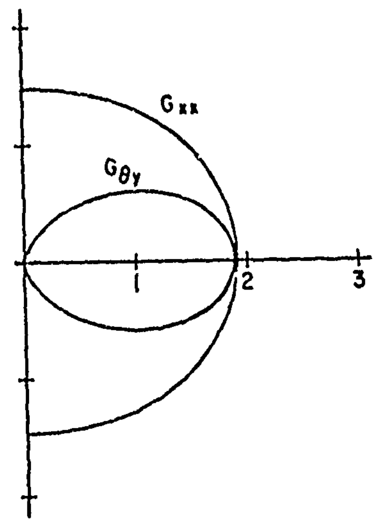

(a) 0.6λ

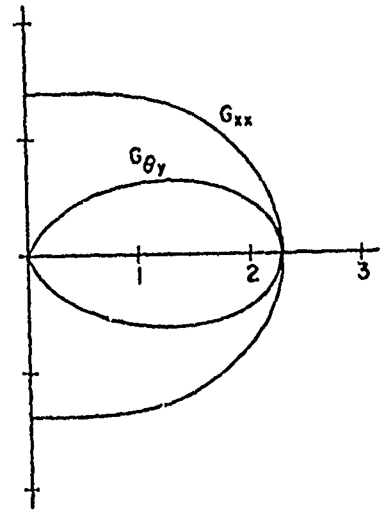

(b) 0.8λ

Fig. 4. Radiation gain patterns for an open-ended rectangular waveguide of dimensions a/b = 2.25 radiating into half space.

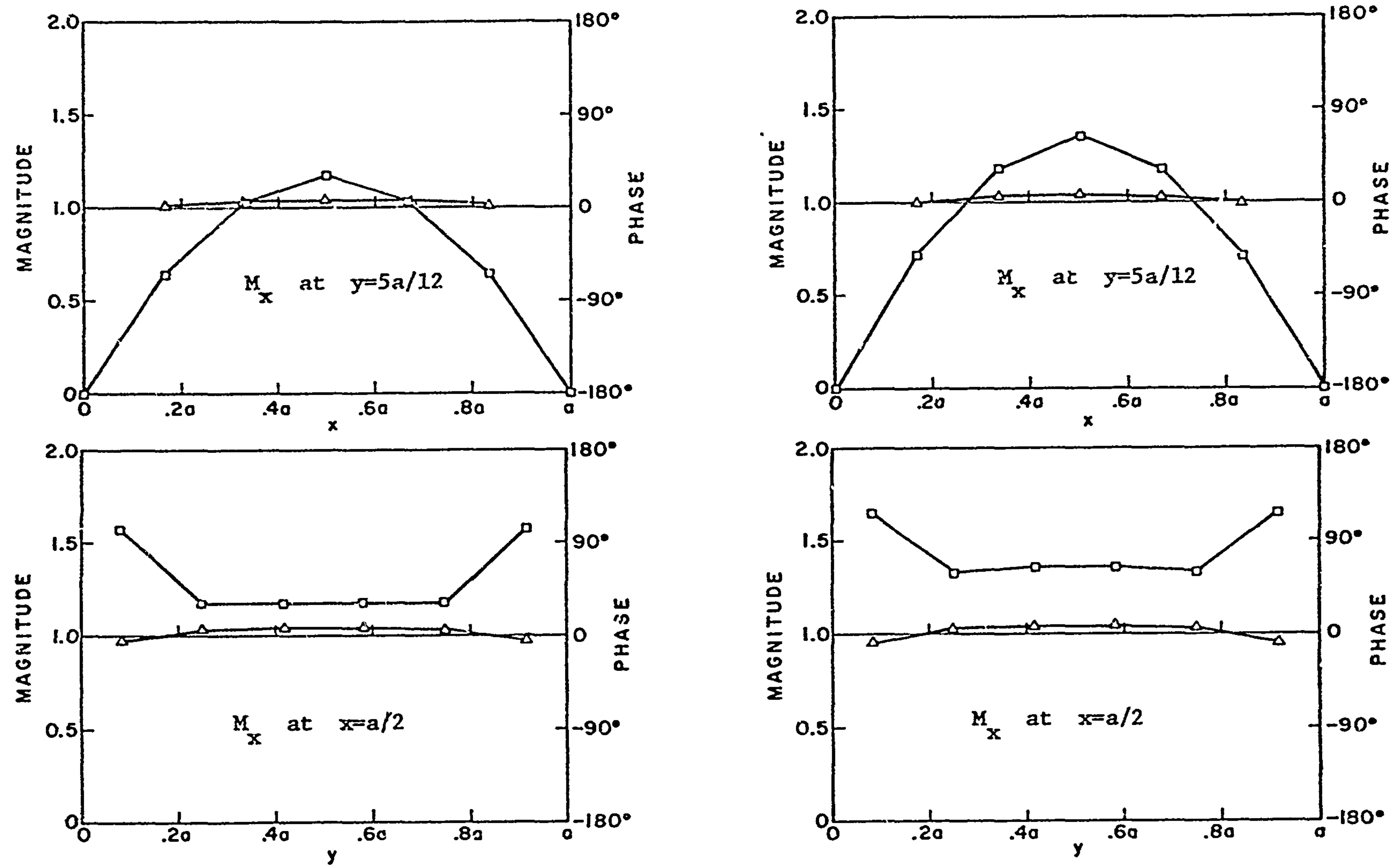

(a) a = 0.6λ

(b) a = 0.8λ

Fig. 5. Equivalent magnetic current for an open-ended square waveguide of width a radiating into half space. Squares denote magnitude, triangles denote phase.

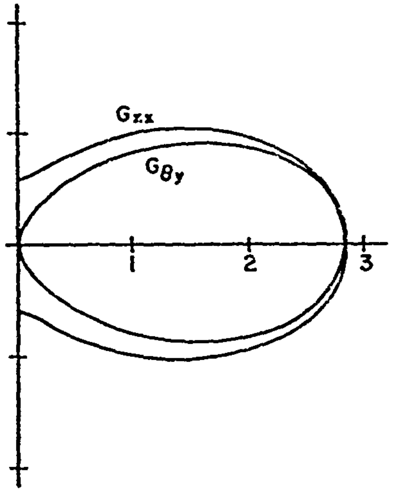

(a) a = 0.6λ

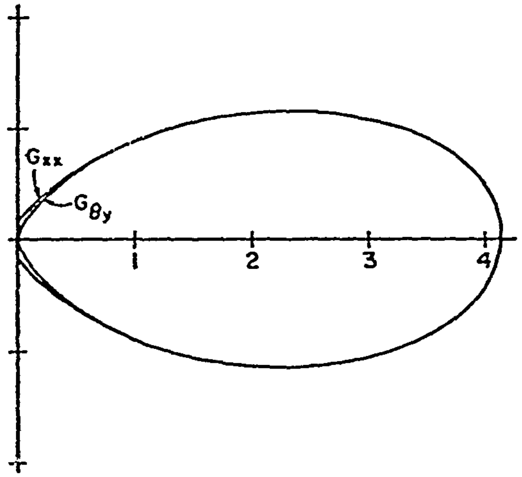

(b) a = 0.8λ

Fig. 6. Radiation gain patterns for an open-ended square waveguide of width a radiating into half space.

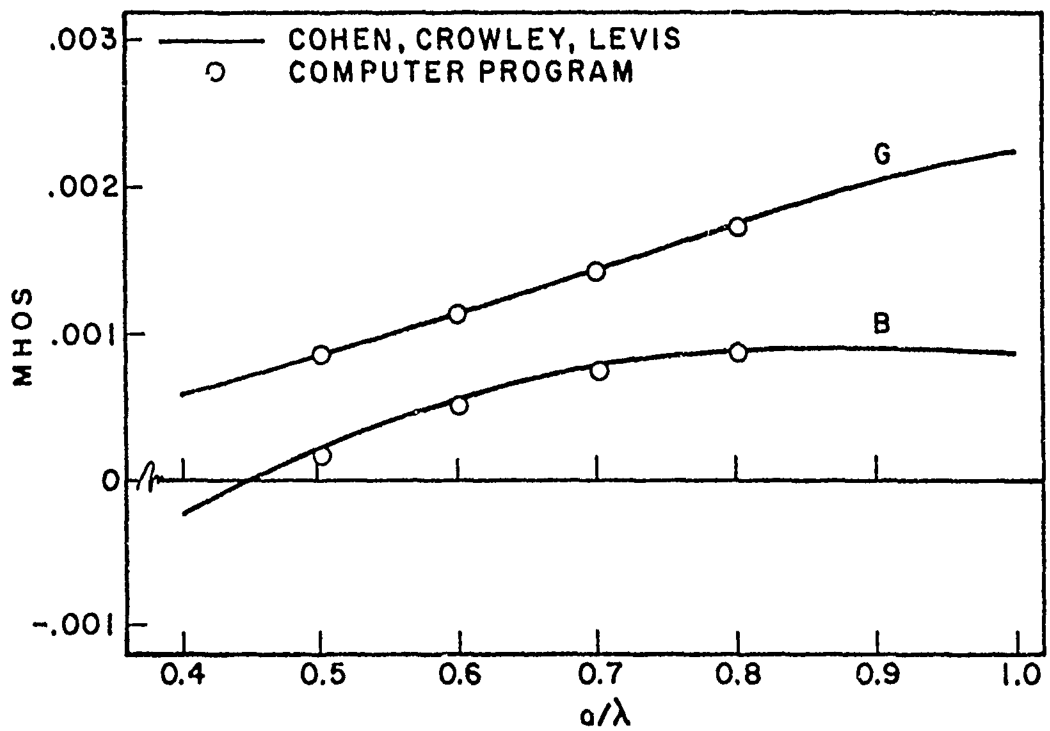

Fig. 7. The equivalent aperture admittance seen by the dominant mode for an open-ended rectangular waveguide of dimensions a/b = 2.25 radiating into half space. Our computed results are compared to those of Cohen, Crowley, and Levis [4].

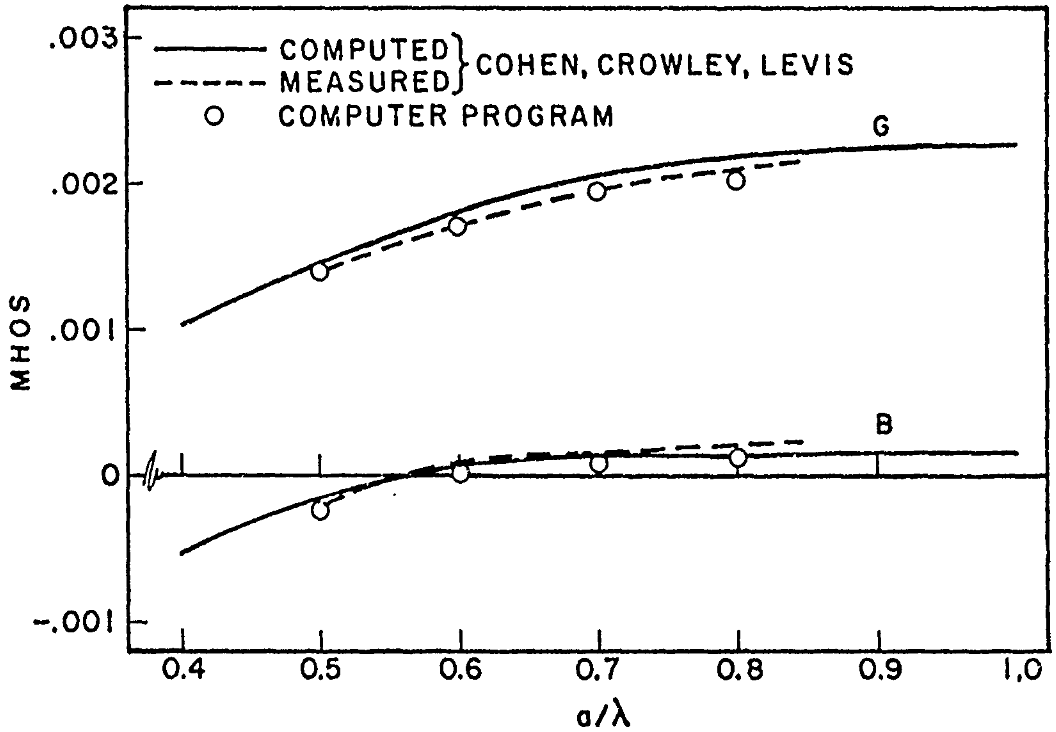

Fig. 8. The equivalent aperture admittance seen by the dominant mode for an open-ended square waveguide of width a radiating into half space. Our computed results are compared to those calculated and measured by Cohen, Crowley, and Levis [4].

Figure 3 shows the equivalent magnetic current for an open-ended rectangular waveguide of dimensions $a/b = 2.25$ radiating into half space, for two different wavelengths. Figure 3(a) is for $a = 0.6\lambda$, and Figure 3(b) is for $a = 0.8\lambda$. Although the aperture is now relatively wide, the y-component of magnetic current is still small, and thus is not shown. The top Figure 3(a) shows magnitude and phase of the x-component of $\underset{\sim}{M}$ at $y = b/2$, and the bottom Figure 3(a) shows them for the x-component of $\underset{\sim}{M}$ at $x = a/2$. The top Figure 3(b) shows the magnitude and phase of the x-component of $\underset{\sim}{M}$ at $y = 3b/8$, and the bottom Figure 3(b) shows them for the x-component of $\underset{\sim}{M}$ at $x = a/2$. Note that M_x is zero at $x = 0$ and $x = a$, and it is large near both $y = 0$ and $y = b$. This is to be expected from theory. Again the magnetic current is normalized according to (68). Figure 4 shows the principal plane radiation patterns for the same waveguide-fed apertures, 4(a) for $a = 0.6\lambda$ and 4(b) for $a = 0.8\lambda$. Again $G_{\theta y}$ denotes the pattern due to H_θ in the $y = 0$ plane, and G_{xx} denotes the pattern due to H_x in the $x = 0$ plane.

Figure 5 shows the equivalent magnetic current for an open-ended square waveguide of side length a radiating into half space, for two different wavelengths. Figure 5(a) is for $a = 0.6\lambda$, and Figure 5(b) is for $a = 0.8\lambda$. The top figures show the magnitude and phase of M_x at $y = 5a/12$, and the bottom figures show them for M_x at $x = a/2$. Again M_x is zero at $x = 0$ and $x = a$, and M_x is large near both $y = 0$ and $y = a$. Figure 6 shows the principal plane radiation gain patterns for the same waveguide-fed apertures, (a) for $a = 0.6\lambda$, and (b) for $a = 0.8\lambda$. Again $G_{\theta y}$ denotes the pattern due to H_θ in the $y = 0$ plane, and G_{xx} denotes the pattern due to H_x in the $x = 0$ plane.

Finally, Figures 7 and 8 show plots of the equivalent aperture admittance seen by the dominant mode for an open-ended waveguide radiating into half space. This aperture admittance is defined by

$$Y_{ap} = \frac{1 - \Gamma_o}{1 + \Gamma_o} Y_o \tag{69}$$

where Γ_o is the reflection coefficient and Y_o is the characteristic wave impedance, both for the dominant mode. Our computations are compared to some previously obtained by Cohen, Crowley, and Levis [4]. Figure 7 shows the results for a rectangular waveguide of dimensions a/b = 2.25, and Figure 8 shows the results for a square waveguide of side length a. Measured results were found only for a square waveguide, and these are also shown in Figure 8.

IX. DISCUSSION

A general purpose computer program has been developed for rectangular waveguides radiating into half space through a rectangular aperture. When the aperture dimensions are small compared to the waveguide dimensions, many waveguide modes may be required to accurately obtain the waveguide admittance matrix. In this case it would be advantageous to have an analytic approximation to the sum of higher-order mode contributions. However, we have not investigated this possibility. Our program appears to give accurate results even for relatively small apertures, although large numbers of higher-order modes may be required.

The numerical examples given in Section VIII serve to illustrate the types of computations that can be made with the general program. The program is written so that the excitation may be any mode desired, not necessarily the dominant mode. The aperture can be located anywhere within the waveguide cross section. The principal limitation to the use of the program is one set by the cross-sectional size (in square wavelengths) of the waveguide and aperture. As with most moment solutions, when the size of the aperture becomes too large then too many expansion functions are required for a solution. As a rule of thumb, for reasonable accuracy we need at least 5 expansion functions per wavelength for each component of current, or 50 expansion functions per square wavelength. Hence, even on large computers, one is limited to apertures of the order of a few square wavelengths in size.

[4] M. Cohen, T. Crowley, K. Levis, "The Aperture Admittance of a Rectangular Waveguide Radiating into Half-Space," Antenna Lab. Rept. ac 21114 S.R. No. 22, Ohio State University, 1953.

PART TWO

COMPUTER PROGRAMS

I. DESCRIPTION OF THE MAIN PROGRAM

The main program computes the complex coefficients V_i which determine the magnetic current M according to (1), the amplitudes Γ_j of (7) of the reflected waveguide modes, the equivalent aperture admittance [1, Eq. (67)] seen by the incident mode, the complex power flowing out of the aperture, and four gain patterns. The four gain patterns are written on the first record of direct access data set 6 so that they may be plotted by the program on pages 43 and 44 of [2]. The main program calls the subroutines AY, YMAT, PLANE, DECOMP and SOLVE which are described in Sections II, III, and IV.

The data cards are read early in the main program according to

```
      READ(1,11) LX, LY, LM, LN, LI, NTH, DX, DY, AL, BL, X1, Y1, ER
   11 FORMAT(6I3, 3E14.7/4E14.7)
```

The variables LX, LY, DX, DY, AL, BL, X1, and Y1 are respectively L_x, L_y, $\Delta x/\lambda$, $\Delta y/\lambda$, a/λ, b/λ, x_1/λ and y_1/λ where λ is the free space wavelength. See Fig. 1. The variables LM and LN are respectively L_m and L_n appearing in (16) and (17). We require that

$$LX \geq 2$$

$$LY \geq 1 \ .$$

The excitation of the waveguide is the LIth waveguide mode where, in the program, $\underset{\sim}{e}^{TE}_{m+n(L_m+1)}$ of (16) is called the $(m+n(L_m+1))$th waveguide mode and $\underset{\sim}{e}^{TM}_{m+(n-1)L_m}$ of (17) is called the $(L_m+L_n(L_m+1) + m + (n-1)L_m)$th waveguide mode. ER is the relative dielectric constant ϵ_r of (31) and (32) inside the waveguide. The four gain patterns are generated by evaluating the plane wave measurement vectors [2, Eqs. (55) to (58)] at angles (θ or ϕ) equal to (J-1)*180./(NTH-1) degrees, J=1,2,...NTH.

PART TWO

COMPUTER PROGRAMS

I. DESCRIPTION OF THE MAIN PROGRAM

The main program computes the complex coefficients V_i which determine the magnetic current M according to (1), the amplitudes Γ_j of (7) of the reflected waveguide modes, the equivalent aperture admittance [1, Eq. (67)] seen by the incident mode, the complex power flowing out of the aperture, and four gain patterns. The four gain patterns are written on the first record of direct access data set 6 so that they may be plotted by the program on pages 43 and 44 of [2]. The main program calls the subroutines AY, YMAT, PLANE, DECOMP and SOLVE which are described in Sections II, III, and IV.

The data cards are read early in the main program according to

```
    READ(1,11) LX, LY, LM, LN, LI, NTH, DX, DY, AL, BL, X1, Y1, ER
11  FORMAT(6I3, 3E14.7/4E14.7)
```

The variables LX, LY, DX, DY, AL, BL, X1, and Y1 are respectively L_x, L_y, $\Delta x/\lambda$, $\Delta y/\lambda$, a/λ, b/λ, x_1/λ and y_1/λ where λ is the free space wavelength. See Fig. 1. The variables LM and LN are respectively L_m and L_n appearing in (16) and (17). We require that

$$LX \geq 2$$

$$LY \geq 1 \; .$$

The excitation of the waveguide is the LIth waveguide mode where, in the program, $\underset{\sim}{e}^{TE}_{m+n(L_m+1)}$ of (16) is called the $(m+n(L_m+1))$th waveguide mode and $\underset{\sim}{e}^{TM}_{m+(n-1)L_m}$ of (17) is called the $(L_m+L_n(L_m+1) + m + (n-1)L_m)$th waveguide mode. ER is the relative dielectric constant ε_r of (31) and (32) inside the waveguide. The four gain patterns are generated by evaluating the plane wave measurement vectors [2, Eqs. (55) to (58)] at angles (θ or ϕ) equal to (J-1)*180./(NTH-1) degrees, J=1,2,...NTH.

Minimum allocations are given by

```
COMPLEX TI(N), GAM(NT), P(4*N), YHS(N*N),
   Y(NT), V(NT), V(N), YWG(N*N)
DIMENSION GA(4*NTH), A(NT*N), IPS(N)
```

in the main program, by

```
COMPLEX Y(NT)
DIMENSION A(N*NT), S1(LMP), S2(LMP), SM(LMP*LX),
    CM(LMP*LX), CN(LNP*LY), SN(LNP*LY)
```

in the subroutine AY, by

```
COMPLEX TC(J1), TX(J1), TY(J1), YXX(J2), Y(N*N)
```

in the subroutine YMAT, by

```
COMPLEX P(4*N)
```

in the subroutine PLANE, by

```
COMPLEX UL(N*N)
DIMENSION SCL(N), IPS(N)
```

in the subroutine DECOMP, and by

```
COMPLEX UL(N*N), B(N), X(N)
DIMENSION IPS(N)
```

in the surboutine SOLVE. Here,

```
N = (LX-1)*LY + LX*(LY-1)
NT = 2*LM*LN + LM + LN
LMP = LM+1
LNP = LN+1
 J1 = (LX+1)*(LY+1)
 J2 = MAX((LX-1)*LY, LX*(LY-1))
```

Referring to (22) to (25), statement 41 stores

$$\sqrt{\frac{2\pi}{\Delta x \Delta y}}\ A_{ij}^{xTE} \text{ in } A(i + (j-1)*N),$$

$$\sqrt{\frac{2\pi}{\Delta x \Delta y}}\ A_{ij}^{yTE} \text{ in } A(NX + i + (j-1)*N),$$

$$\sqrt{\frac{2\pi}{\Delta x \Delta y}}\ A_{ij}^{xTM} \text{ in } A(N*NTE + i + (j-1)*N), \text{ and}$$

$$\sqrt{\frac{2\pi}{\Delta x \Delta y}}\ A_{ij}^{yTM} \text{ in } A(NX + N*NTE + i + (j-1)*N)$$

where

N = (LX-1)*LY + LX*(LY-1)

NX = (LX-1)*LY

NTE = LM*LN + LM + LN

With regard to (31) and (32), statement 41 also stores $-j\eta Y_j^{TE}$ in Y(j) and $-j\eta Y_j^{TM}$ in Y(NTE+j). Statement 42 stores $\frac{2\pi\eta}{j\Delta x\Delta y}\ Y^{hs}$ by columns in YHS where the set of expansion functions $\underset{\sim}{M}_i$ appearing in the definition (3) of Y^{hs} is $\underset{\sim}{M}_j^y$ of (11) appended to $\underset{\sim}{M}_j^x$ of (10).

[illegible]rning (2), nested DO loops 13 and 15 store the (I,J)th and (J,I)th elem[illegible] assumed to be equal, of $\frac{2\pi\eta}{j\Delta x\Delta y}\,[Y^{wg} + Y^{hs}]$ in YWG(J2) and YWG(J3). DO loop 14 puts $Y_I A_{JI}$ of (4) in V(I). In DO loop 16, K is the summation index n in (4). Just after exit from DO loop 15, the Jth element of $-j\eta\sqrt{\frac{2\pi}{\Delta x\Delta y}}\ \vec{I}^{\,i}$ is put in TI(J). Statements 43 and 44 store $\sqrt{\frac{\Delta x\Delta y}{2\pi}}\ \vec{V}$ in V.

Inner DO loop 20 accumulates the left-hand side of (7), namely

$$1 + \Gamma_I \quad , \quad I = LI$$

$$\Gamma_I \quad , \quad I \neq LI$$

in U1 where the subscript 0 in (7) is being interpreted as LI. Outer DO loop 19 accumulates

$$-j\eta|1 + \Gamma_{LI}|^2 \, Y_{LI} - j\eta \sum_{I \neq LI} Y_I |\Gamma_I|^2$$

in U2. Statement 45 puts ηP_{wg} where P_{wg} is given by (62) in U2.

From [1, Eqs. (45) and (48)],

$$\iint_{\text{guide}} |\underset{\sim}{E}_t^i|^2 ds = 1$$

where $\underset{\sim}{E}_t^i$ is the transverse electric field of the forward traveling (incident) mode at z = 0. Hence expression (68) reduces to $\frac{1}{\sqrt{ab}}$.

The V which is printed upon exit from DO loop 34 is $\sqrt{ab}\,\vec{V}$. Statement 46 puts Y_{ap} of [1, Eq. (67)] in U1.

Concerning (59), Nested DO loops 23 and 24 accumulate $\frac{2\pi j\eta ab}{\Delta x \Delta y}$ $\tilde{V}Y^{hs*}\vec{V}^*$ in U2. Statement 47 puts $\eta\tilde{V}Y^{hs*}\vec{V}^*$ in U1.

Do loop 26 stores G of (8) in G(K). Statement 27 uses TH = (J-1*π/(NTH-1) radians to store $\frac{1}{2\Delta x \Delta y} P_i^m$ in P(i + (K-1)*N). P_i^m is given by [2, Eq. (54 + K)] where θ or ϕ is TH. For the $\frac{1}{2\Delta x \Delta y} \vec{P}^m$ stored in P(1 + (K-1)*N) through P(K*N), DO loop 29 accumulates $\frac{\sqrt{ab}}{2\Delta x \Delta y} \tilde{P}^m \vec{V}$ in U1. Next, G of (8) is stored in both G(K) and GA(J + (K-1)*NTH).

Statement 32 writes GA on the first record of data set 6 for possible input to the plot program listed in [2, pages 43-44].

```
C      LISTING OF THE MAIN PROGRAM AND SAMPLE DATA
C
// EXEC WATFIV
//GO.FT06F001 DD DSNAME=EE0034.REV1,DISP=OLD,UNIT=3330,                     X
//              DCB=(RECFM=VS,BLKSIZE=2596,LRECL=2592)
//GO.SYSIN DD *
$JOB            MAUTZ,TIME=1,PAGES=40
C
C      MAIN PROGRAM
C      THIS PROGRAM CALLS THE SUBROUTINES AY,YMAT,PLANE,DECOMP,SOLVE
       COMPLEX TI(50),GAM(400),P(200),CONJG
       COMPLEX YHS(2500),Y(400),U2,V(400),U1,YWG(2500)
       DIMENSION G(4),GA(1168),A(2500),IPS(50)
       REWIND 6
       READ(1,11) LX,LY,LM,LN,LI,NTH,DX,DY,AL,BL,X1,Y1,ER
    11 FORMAT(6I3,3F14.7/4E14.7)
       WRITE(3,12) LX,LY,LM,LN,LI,NTH,DX,DY,AL,BL,X1,Y1,ER
    12 FORMAT('  LX LY LM LN LI NTH',5X,'DX',12X,'DY',12X,'AL'/1X,6I3,
      13E14.7/7X,'BL',12X,'X1',12X,'Y1',12X,'ER'/1X,4E14.7)
       PI=3.141593
       P2=2.*PI
       DX=DX*P2
       DY=DY*P2
       X1=X1*P2
       Y1=Y1*P2
       AL=.5/AL
       BL=.5/BL
    41 CALL AY(LX,LY,LM,LN,DX,DY,AL,BL,X1,Y1,ER,A,Y)
    42 CALL YMAT(LX,LY,DX,DY,YHS)
       N=(LX-1)*LY+LX*(LY-1)
       NT=2*LM*LN+LN+LM
       U2=2.*Y(LI)
       J2=1
       J5=N*(LI-1)
       DO 13 J=1,N
       J1=J
       DO 14 I=1,NT
       V(I)=Y(I)*A(J1)
       J1=J1+N
    14 CONTINUE
       J3=J2
       DO 15 I=J,N
       U1=YHS(J2)
       J4=I
       DO 16 K=1,NT
       U1=U1+A(J4)*V(K)
       J4=J4+N
    16 CONTINUE
       YWG(J2)=U1
       YWG(J3)=U1
       J2=J2+1
       J3=J3+N
    15 CONTINUE
       J2=J2+J
       J5=J5+1
       TI(J)=U2*A(J5)
    13 CONTINUE
    43 CALL DECOMP(N,IPS,YWG)
    44 CALL SOLVE(N,IPS,YWG,TI,V)
       J1=0
```

```
      U2=0.
      DO 19 I=1,NT
      U1=0.
      DO 20 J=1,N
      J1=J1+1
      U1=U1+A(J1)*V(J)
   20 CONTINUE
      U2=U2+U1*CONJG(U1)*Y(I)
      GAM(I)=U1
   19 CONTINUE
   45 U2=(0.,1.)*(CONJG(U2)-2.*GAM(LI)*CONJG(Y(LI)))
      GAM(LI)=GAM(LI)-1.
      CV=PI*SQRT(P2/(AL*BL*DX*DY))
      DO 34 I=1,N
      V(I)=CV*V(I)
   34 CONTINUE
      WRITE(3,35)(V(I),I=1,N)
   35 FORMAT(' COEFFICIENTS V DIVIDED BY RMS INCIDENT E OVER',
     1' GUIDE CROSS SECTION'/(1X,6E11.4))
      WRITE(3,33)(GAM(I),I=1,NT)
   33 FORMAT('0AMPLITUDES OF REFLECTED WAVEGUIDE MODES'/(1X,6E11.4))
   46 U1=(1./376.730)*(0.,1.)*Y(LI)*(1.-GAM(LI))/(1.+GAM(LI))
      WRITE(3,36) U1
   36 FORMAT('0EQUIVALENT APERTURE ADMITTANCE OF INCIDENT MODE=',2E11.4)
      WRITE(3,40) U2
   40 FORMAT('0(COMPLEX WAVEGUIDE POWER)*ETA=',2E11.4)
      U2=0.
      DO 23 I=1,N
      U1=0.
      J1=I
      DO 24 J=1,N
      U1=U1+YHS(J1)*V(J)
      J1=J1+N
   24 CONTINUE
      U2=U2+V(I)*CONJG(U1)
   23 CONTINUE
   47 U1=-1./(CV*CV)*(0.,1.)*U2
      WRITE(3,39) U1
   39 FORMAT('0(COMPLEX HALF SPACE POWER)*ETA=',2E11.4)
      CG=DX*DY/AIMAG(U2)
      DTH=PI/(NTH-1)
      P8=180./PI
      WRITE(3,25)
   25 FORMAT('0 ANGLE',5X,'G1',9X,'G2',9X,'G3',9X,'G4')
      DO 26 J=1,NTH
      TH=(J-1)*DTH
   27 CALL PLANE(TH,LX,LY,DX,DY,P)
      TH=TH*P8
      J1=0
      J2=J
      DO 28 K=1,4
      U1=0.
      DO 29 I=1,N
      J1=J1+1
      U1=U1+P(J1)*V(I)
   29 CONTINUE
      H=U1*CONJG(U1)
      G(K)=CG*H
      GA(J2)=G(K)
      J2=J2+NTH
```

```
   28 CONTINUE
      WRITE(3,30) TH,(G(I),I=1,4)
   30 FORMAT(1X,F7.2,4E11.4)
   26 CONTINUE
      KA=J2-NTH
   32 WRITE(6)(GA(J),J=1,KA)
      STOP
      END
$DATA
  5  1  9  0  1 19 0.5000000E-01 0.5000000E-01 0.2500000E+00
 0.5000000F-01 0.0000000E+00 0.0000000E+00 0.1000000E+01
$STOP
/*
//
```

PRINTED OUTPUT

```
 LX LY LM LN LI NTH      DX              DY              AL
  5  1  9  0  1 19 0.5000000E-01 0.5000000E-01 0.2500000E+00
      BL            X1              Y1              ER
 0.5000000F-01 0.0000000E+00 0.0000000F+00 0.1000000E+00
COEFFICIENTS V DIVIDED BY RMS INCIDENT E OVER GUIDE CROSS SECTION
 0.1336E+01-0.2699E-01 0.2079E+01-0.3602E-01 0.2079E+01-0.3602E-01
 0.1336E+01-0.2699E-01

AMPLITUDES OF REFLECTED WAVEGUIDE MODES
 0.5121E+00-0.2743E-01-0.4172E-06 0.1863E-07 0.2043E-01-0.1874E-02
 0.7153E-06-0.1211E-07-0.6584E-06 0.1307E-07 0.4098E-06-0.9080E-08
-0.3752E-02 0.3443E-03-0.4098E-07 0.2328E-09-0.1867E-01 0.3387E-03

EQUIVALENT APERTURE ADMITTANCE OF INCIDENT MODE= 0.1103E-03-0.1481E-02

(COMPLEX WAVEGUIDE POWER)*ETA= 0.9504E-01 0.1268E+01

(COMPLEX HALF SPACE POWER)*ETA= 0.9504E-01 0.1268E+01

 ANGLE      G1          G2          G3          G4
   0.00 0.0000E+00 0.0000E+00 0.0000E+00 0.1530E+01
  10.00 0.4144E-01 0.0000E+00 0.0000E+00 0.1531E+01
  20.00 0.1625E+00 0.0000E+00 0.0000E+00 0.1532E+01
  30.00 0.3528E+00 0.0000E+00 0.0000E+00 0.1533E+01
  40.00 0.5945E+00 0.0000E+00 0.0000E+00 0.1536E+01
  50.00 0.8621E+00 0.0000E+00 0.0000E+00 0.1538E+01
  60.00 0.1123E+01 0.0000E+00 0.0000E+00 0.1540E+01
  70.00 0.1344E+01 0.0000E+00 0.0000E+00 0.1541E+01
  80.00 0.1491E+01 0.0000E+00 0.0000E+00 0.1543E+01
  90.00 0.1543E+01 0.0000E+00 0.0000E+00 0.1543E+01
 100.00 0.1491E+01 0.0000E+00 0.0000E+00 0.1543E+01
 110.00 0.1344E+01 0.0000E+00 0.0000E+00 0.1541E+01
 120.00 0.1123E+01 0.0000E+00 0.0000E+00 0.1540E+01
 130.00 0.8621E+00 0.0000E+00 0.0000E+00 0.1538E+01
 140.00 0.5945E+00 0.0000E+00 0.0000E+00 0.1536E+01
 150.00 0.3528E+00 0.0000E+00 0.0000E+00 0.1533E+01
 160.00 0.1625E+00 0.0000E+00 0.0000E+00 0.1532E+01
 170.00 0.4144E-01 0.0000E+00 0.0000E+00 0.1531E+01
 180.00 0.5398E-12 0.0000E+00 0.0000F+00 0.1530E+01
```

II. DESCRIPTION OF THE SUBROUTINE AY

The subroutine AY(LX, LY, LM, LN, DX, DY, AL, BL, X1, Y1, ER, A,Y) stores the submatrices defined by (22) to (25) in A and the admittances defined by (31) and (32) in Y. More precisely,

$$\sqrt{\frac{2\pi}{\Delta x \Delta y}}\ A^{xTE}_{ij} \text{ is stored in A(i + (j-1)*N),}$$

$$\sqrt{\frac{2\pi}{\Delta x \Delta y}}\ A^{yTE}_{ij} \text{ is stored in A(NX + i + (J-1)*N),}$$

$$\sqrt{\frac{2\pi}{\Delta x \Delta y}}\ A^{xTM}_{ij} \text{ is stored in A(N*NTE + i + (j-1)*N), and}$$

$$\sqrt{\frac{2\pi}{\Delta x \Delta y}}\ A^{yTM}_{ij} \text{ is stored in A(NX + N*NTE + i + (j-1)*N)}$$

where

NX = (LX - 1)*LY

N = NX + LX*(LY-1)

NTE = LM*LN + LM + LN.

Also,

$-j\eta Y^{TE}_{j}$ is stored in Y(j) and

$-j\eta Y^{TM}_{j}$ is stored in Y(NTE + j).

The values of the variables in (22) to (32) are specified by the first eleven arguments of AY.

ARGUMENT OF AY	VARIABLE IN (22) TO (32)
LX	L_x
LY	L_y
LM	L_m
LN	L_n
DX	$k\Delta x$
DY	$k\Delta y$
AL	$\pi/(ka)$
BL	$\pi/(kb)$
X1	kx_1
Y1	ky_1
ER	ε_r

Minimum allocations are given by

```
COMPLEX Y(NT)
DIMENSION A(N*NT), S1(LMP), S2(LMP), SM(LMP*LX)
    CM(LMP*LX), CN(LNP*LY), SN(LNP*LY)
```

where

```
  N = (LX-1)*LY + LX * (LY-1)
LMP = LM + 1
LNP = LN + 1
 NT = 2*LM*LN + LM + LN .
```

Statement 32 stores $\sqrt{\frac{8\pi\Delta x\Delta y}{ab}}$ in C. DO loop 10 stores

$$\sqrt{\frac{8\pi\Delta x\Delta y}{ab}}\left(\frac{\sin\frac{m\pi\Delta x}{2a}}{\frac{m\pi\Delta x}{2a}}\right)^2 \frac{m\pi}{k\varepsilon} \text{ in S1(m+1), and}$$

$$\sqrt{\frac{4\pi\Delta x\Delta y\varepsilon_m}{ab}}\left(\frac{\sin\frac{m\pi\Delta x}{2a}}{\frac{m\pi\Delta x}{2a}}\right) \text{ in S2(m + 1)}$$

whereas nested DO loops 10 and 12 store

$$\sin \frac{m\pi(x_1 + p\Delta x)}{a} \text{ in SM(m+1 + }(L_m + 1)\text{*p), and}$$

$$\cos \frac{m\pi(x_1 + (p - \frac{1}{2})\Delta x)}{a} \text{ in CM (m + 1 + }(L_m + 1)\text{*p).}$$

In DO loops 10 and 12, JM corresponds to m+1 and JP to p. Nested DO loops 13 and 14 store

$$\sin \frac{n\pi(y_1 + q\Delta y)}{b} \text{ in SN(n + 1 }(L_n + 1)\text{*q), and}$$

$$\cos \frac{n\pi(y_1 + (q - \frac{1}{2})\Delta y)}{b} \text{ in CN(n + 1 + }(L_n + 1)\text{*q).}$$

In DO loops 13 and 14, JN corresponds to n+1 and JQ to q.

DO loop 16 stores (22) to (25) in A. The DO loop indices JN, JM, JP, and JQ are equal to n+1, m+1, p, and q respectively. Just before DO loop 20 is entered,

$$C1 = \sqrt{\frac{\varepsilon_n}{2}} \; \frac{\sin \frac{n\pi\Delta y}{2b}}{\frac{n\pi\Delta y}{2b}}$$

$$C2 = \frac{n\pi}{kb} \left(\frac{\sin \frac{n\pi\Delta y}{2b}}{\frac{n\pi\Delta y}{2b}} \right)^2 .$$

Statement 27 or 29 stores $-j\eta Y^{TE}$ of (31) in Y. If the calculated value of

$(\frac{k_1}{k})^2 - \varepsilon_r$ is zero, then statement 28 replaces

$(\frac{k_1}{k})^2 - \varepsilon_r$ by 10^{-6} ε_r. Just before DO loop 21 is entered,

$$C3 = \sqrt{\frac{4\pi\Delta x\Delta y\epsilon_n}{ab}}\left(\frac{m\pi}{k_j a}\right)\left(\frac{\sin\frac{m\pi\Delta x}{2a}}{\frac{m\pi\Delta x}{2a}}\right)^2\left(\frac{\sin\frac{n\pi\Delta y}{2b}}{\frac{n\pi\Delta y}{2b}}\right)$$

$$C4 = \sqrt{\frac{4\pi\Delta x\Delta y\epsilon_m}{ab}}\left(\frac{n\pi}{k_j b}\right)\left(\frac{\sin\frac{n\pi\Delta y}{2b}}{\frac{n\pi\Delta y}{2b}}\right)^2\left(\frac{\sin\frac{m\pi\Delta x}{2a}}{\frac{m\pi\Delta x}{2a}}\right) .$$

Nested DO loops 21 and 22 store $\sqrt{\frac{2\pi}{\Delta x\Delta y}}\ A^{xTE}$ of (22) in A. Nested DO loops 23 and 24 store $\sqrt{\frac{2\pi}{\Delta x\Delta y}}\ A^{yTE}$ of (23) in A. Statement 33 stores $-j\eta Y^{TM}$ of (32) in Y. DO loop 25 stores $\sqrt{\frac{2\pi}{\Delta x\Delta y}}\ A^{xTM}$ of (24) in A. DO loop 26 stores $\sqrt{\frac{2\pi}{\Delta x\Delta y}}\ A^{yTM}$ of (25) in A.

```
C     LISTING OF THE SUBROUTINE AY
C
      SUBROUTINE AY(LX,LY,LM,LN,DX,DY,AL,BL,X1,Y1,ER,A,Y)
      COMPLEX U,Y(400)
      DIMENSION A(2500),S1(40),S2(40),SM(400),CM(400),CN(100),SN(100)
      U=(0.,1.)
   32 C=SQRT(2.546479*DX*DY*AL*BL)
      DX5=.5*DX
      LMP=LM+1
      S1(1)=0.
      S2(1)=.7071068*C
      DO 10 JM=1,LMP
      AM=(JM-1)*AL
      DXM=DX5*AM
      IF(JM.EQ.1) GO TO 11
      C1=SIN(DXM)/DXM
      S2(JM)=C*C1
      S1(JM)=S2(JM)*C1*AM
   11 J1=JM
      DO 12 JP=1,LX
      C1=(X1+JP*DX)*AM
      C2=C1-DXM
      SM(J1)=SIN(C1)
      CM(J1)=COS(C2)
      J1=J1+LMP
   12 CONTINUE
   10 CONTINUE
      DY5=.5*DY
      LNP=LN+1
      DO 13 JN=1,LNP
      BN=(JN-1)*BL
      DYM=DY5*BN
      J1=JN
      DO 14 JQ=1,LY
      C1=(Y1+JQ*DY)*BN
      C2=C1-DYM
      SN(J1)=SIN(C1)
      CN(J1)=COS(C2)
      J1=J1+LNP
   14 CONTINUE
   13 CONTINUE
      LXM=LX-1
      LYM=LY-1
      NX=LXM*LY
      NY=LX*LYM
      N=NX+NY
      JTE=0
      JTM=N*(LNP*LMP-1)
      KTE=0
      KTM=LNP*LMP-1
      C1=.7071068
      C2=0.
      DO 16 JN=1,LNP
      BN=(JN-1)*BL
      BN2=BN*BN
      IF(JN.EQ.1) GO TO 19
      X=BN*DY5
      C1=SIN(X)/X
      C2=C1*C1*BN
   19 DO 20 JM=1,LMP
```

```
      IF((JN+JM).EQ.2) GO TO 20
      AM=(JM-1)*AL
      C7=BN2+AM*AM
      C8=SQRT(C7)
      C7=C7-ER
      KTE=KTE+1
      IF(C7) 27,28,29
   27 Y(KTE)=-U*SQRT(-C7)
      GO TO 30
   28 C7=1.E-6*ER
   29 Y(KTE)=-SQRT(C7)
   30 C3=S1(JM)*C1/C8
      C4=S2(JM)*C2/C8
      J1=JN
      DO 21 JQ=1,LY
      C5=C3*CN(J1)
      J1=J1+LNP
      J2=JM
      DO 22 JP=1,LXM
      JTE=JTE+1
      A(JTE)=C5*SM(J2)
      J2=J2+LMP
   22 CONTINUE
   21 CONTINUE
      GO TO (31), LY
      J1=JN
      DO 23 JQ=1,LYM
      C5=C4*SN(J1)
      J1=J1+LNP
      J2=JM
      DO 24 JP=1,LX
      JTE=JTE+1
      A(JTE)=C5*CM(J2)
      J2=J2+LMP
   24 CONTINUE
   23 CONTINUE
   31 IF((JN-1)*(JM-1).EQ.0) GO TO 20
      KTM=KTM+1
   33 Y(KTM)=-ER/Y(KTE)
      C5=BN/AM
      J1=JTE-N
      DO 25 J=1,NX
      JTM=JTM+1
      J1=J1+1
      A(JTM)=-C5*A(J1)
   25 CONTINUE
      GO TO (20), LY
      C5=AM/BN
      DO 26 J=1,NY
      JTM=JTM+1
      J1=J1+1
      A(JTM)=C5*A(J1)
   26 CONTINUE
   20 CONTINUE
   16 CONTINUE
      RETURN
      END
```

III. THE SUBROUTINES YMAT AND PLANE

THE SUBROUTINES YMAT AND PLANE ARE DESCRIBED ON PAGES 30 TO 41 OF REFERENCE 2.

```
C     LISTINGS OF THE SUBROUTINES YMAT AND PLANE
C
      SUBROUTINE YMAT(LX,LY,DX,DY,Y)
      COMPLEX U,U1,U2,U3,U4,EX,TC(100),TX(100),TY(100),YXX(100),Y(2500)
      DX2=1./(DX*DX)
      DY2=1./(DY*DY)
      DXDY=DX*DY
      NX=(LX-1)*LY
      NY=(LY-1)*LX
      N=NX+NY
      LXP=LX+1
      LYP=LY+1
      LXM=LX-1
      LYM=LY-1
      U=(0.,1.)
      U4=.1666667*U
      JST=LX+1
      DO 15 JT=1,LY
      JST=JST+1
      YL=(JT-1.5)*DY
      YU=YL+DY
      YL2=YL*YL
      YU2=YU*YU
      Y1=(JT-1)*DY
      Y2=Y1*Y1
      DO 16 JS=1,LX
      XL=(JS-1.5)*DX
      XU=XL+DX
      XL2=XL*XL
      XU2=XU*XU
      X1=(JS-1)*DX
      X2=X1*X1
      R2=X2+Y2
      R1=SQRT(R2)
      RU1=1.-.5*R2
      U1=RU1+R1*(1.-.1666667*R2)*U
      U2=R1-RU1*U
      U3=-.5-.5*R1*U
      EX=COS(R1)-U*SIN(R1)
      JST=JST+1
      R5=XL2+YL2
      R6=XU2+YL2
      R7=XL2+YU2
      R8=XU2+YU2
      R1=SQRT(R5)
      R2=SQRT(R6)
      R3=SQRT(R7)
      R4=SQRT(R8)
      AYL=YL*ALOG((XU+R2)/(XL+R1))
      AYU=YU*ALOG((XU+R4)/(XL+R3))
      AXL=XL*ALOG((YU+R3)/(YL+R1))
      AXU=XU*ALOG((YU+R4)/(YL+R2))
      S1=AXU-AXL+AYU-AYL
      AYL=YL*AYL
```

```
      AYU=YU*AYU
      AXL=XL*AXL
      AXU=XU*AXU
      S3=XU*AXU-XL*AXL+YU*AYU-YL*AYL
      XY1=XL*YL
      XY2=XU*YL
      XY3=XL*YU
      XY4=XU*YU
      S5=.3333333*(XY4*R4-XY3*R3-XY2*R2+XY1*R1)+.1666667*S3
      TC(JST)=(S1*U1+DXDY*U2+S5*U3+.3333333*(XY4*R8-XY3*R7-XY2*R6+XY1*R5
     1)*U4)*EX
      YR1=YL*R1
      YR2=YL*R2
      YR3=YU*R3
      YR4=YU*R4
      S5=.8333333E-1*(YR4*R8-YR3*R7-YR2*R6+YR1*R5)+.125*(XU2*(YR4-YR2)-X
     1L2*(YR3-YR1)+XU2*AXU-XL2*AXL)
      S6=.25*DY*(XU2*XU2-XL2*XL2)+.3333333*X1*DX*(YU2*YU-YL2*YL)
      TX(JST)=.5*(YR4-YR3-YR2+YR1+AXU-AXL)*U1+X1*DXDY*U2+S5*U3+S6*U4
      TX(JST)=TX(JST)*EX/DX
      XR1=XL*R1
      XR2=XU*R2
      XR3=XL*R3
      XR4=XU*R4
      S5=.8333333E-1*(XR4*R8-XR3*R7-XR2*R6+XR1*R5)+.125*(YU2*(XR4-XR3)-Y
     1L2*(XR2-XR1)+YU2*AYU-YL2*AYL)
      S6=.25*DX*(YU2*YU2-YL2*YL2)+.3333333*Y1*DY*(XU2*XU-XL2*XL)
      TY(JST)=.5*(XR4-XR3-XR2+XR1+AYU-AYL)*U1+Y1*DXDY*U2+S5*U3+S6*U4
      TY(JST)=TY(JST)*EX/DY
   16 CONTINUE
   15 CONTINUE
      IF(LYM) 44,44,45
   44 J1=LXP+1
      J2=J1+2
      TC(J1)=TC(J2)
      TX(J1)=-TX(J2)
      TY(J1)=TY(J2)
      GO TO 46
   45 J1=2*LXP+1
      DO 17 JS=2,LXP
      J1=J1+1
      TC(JS)=TC(J1)
      TX(JS)=TX(J1)
      TY(JS)=-TY(J1)
   17 CONTINUE
      J1=1
      DO 18 JT=1,LYP
      J2=J1+2
      TC(J1)=TC(J2)
      TX(J1)=-TX(J2)
      TY(J1)=TY(J2)
      J1=J1+LXP
   18 CONTINUE
   46 J4=LX+2
      JY=0
      DO 19 JT=2,LYP
      DO 20 JS=2,LX
      J3=J4
      J4=J4+1
      J5=J4+1
```

```
      JY=JY+1
      YXX(JY)=.5*(TC(J4)+(JS-.5)*TC(J5)-(JS-3.5)*TC(J3)-TX(J5)+TX(J3))+D
     1X2*(TC(J5)-2.*TC(J4)+TC(J3))
   20 CONTINUE
      J4=J4+2
   19 CONTINUE
      JY=0
      DO 24 JT=1,LY
      DO 23 JS=1,LXM
      DO 22 JQ=1,LY
      JTQ=LXM*IABS(JT-JQ)+1
      DO 21 JP=1,LXM
      J1=JTQ+IABS(JS-JP)
      JY=JY+1
      Y(JY)=YXX(J1)
   21 CONTINUE
   22 CONTINUE
      JY=JY+NY
   23 CONTINUE
   24 CONTINUE
      IF(LYM.EQ.0) RETURN
      J4=2*LXP+1
      JY=0
      DO 25 JT=3,LYP
      DO 26 JS=2,LX
      JY=JY+1
      J4=J4+1
      J3=J4-LXP
      YXX(JY)=(-TC(J4)+TC(J3)+TC(J4+1)-TC(J3+1))/DXDY
   26 CONTINUE
      J4=J4+2
   25 CONTINUE
      JY=NX
      DO 30 JT=1,LY
      DO 29 JS=1,LXM
      DO 28 JQ=1,LYM
      JTQ=2*(JT-JQ)-1
      J2=LXM*(IABS(JTQ)-1)/2
      DO 27 JP=1,LX
      JSP=2*(JS-JP)+1
      J1=J2+(IABS(JSP)+1)/2
      JY=JY+1
      Y(JY)=YXX(J1)
      IF(JTQ*JSP.LT.0) Y(JY)=-Y(JY)
   27 CONTINUE
   28 CONTINUE
      JY=JY+NX
   29 CONTINUE
   30 CONTINUE
      JY=0
      J4=LXP+2
      DO 31 JT=2,LY
      DO 32 JS=3,LXP
      J3=J4
      J4=J4+1
      J5=J4+LXP
      JY=JY+1
      YXX(JY)=(-TC(J4)+TC(J3)+TC(J5)-TC(J5-1))/DXDY
   32 CONTINUE
      J4=J4+2
```

```
31 CONTINUE
   JY=N*NX
   DO 36 JT=1,LYM
   DO 35 JS=1,LX
   DO 34 JQ=1,LY
   JTQ=2*(JT-JQ)+1
   J2=LXM*(IABS(JTQ)-1)/2
   DO 33 JP=1,LXM
   JY=JY+1
   JSP=2*(JS-JP)-1
   J1=J2+(IABS(JSP)+1)/2
   Y(JY)=YXX(J1)
   IF(JTQ*JSP.LT.0) Y(JY)=-Y(JY)
33 CONTINUE
34 CONTINUE
   JY=JY+NY
35 CONTINUE
36 CONTINUE
   JY=0
   J4=LX+2
   DO 37 JT=2,LY
   DO 38 JS=2,LXP
   JY=JY+1
   J4=J4+1
   J5=J4+LXP
   J3=J4-LXP
   YXX(JY)=.5*(TC(J4)+(JT-.5)*TC(J5)-(JT-3.5)*TC(J3)-TY(J5)+TY(J3))+D
  1Y2*(TC(J5)-2.*TC(J4)+TC(J3))
38 CONTINUE
   J4=J4+1
37 CONTINUE
   JY=(N+1)*NX
   DO 42 JT=1,LYM
   DO 41 JS=1,LX
   DO 40 JQ=1,LYM
   JTQ=LX*IABS(JT-JQ)+1
   DO 39 JP=1,LX
   J1=JTQ+IABS(JS-JP)
   JY=JY+1
   Y(JY)=YXX(J1)
39 CONTINUE
40 CONTINUE
   JY=JY+NX
41 CONTINUE
42 CONTINUE
   RETURN
   END
   SUBROUTINE PLANE(TH,LX,LY,DX,DY,P)
   COMPLEX U,U1,P(200)
   U=(0.,1.)
   LXM=LX-1
   LYM=LY-1
   NX=LXM*LY
   N=NX+LYM*LX
   N4=N*4
   DO 89 J=1,N4
   P(J)=0.
89 CONTINUE
   SN=SIN(TH)
   CS=COS(TH)
```

```
      X2=DX*CS
      X3=.5*X2
      S1=-SIN(X3)/X3
      S2=S1*S1*SN
      DO 81 JP=1,LXM
      S5=JP*X2
      U1=S2*(COS(S5)+U*SIN(S5))
      J1=JP
      DO 87 JQ=1,LY
      P(J1)=U1
      J1=J1+LXM
   87 CONTINUE
   81 CONTINUE
      IF(LYM.EQ.0) GO TO 90
      DO 82 JP=1,LX
      S5=(JP-.5)*X2
      U1=S1*(COS(S5)+U*SIN(S5))
      J1=N+NX+JP
      DO 88 JQ=1,LYM
      P(J1)=U1
      J1=J1+LX
   88 CONTINUE
   82 CONTINUE
   90 Y2=DY*CS
      Y3=.5*Y2
      S1=-SIN(Y3)/Y3
      S2=S1*S1*SN
      J1=2*N+NX
      IF(LYM.EQ.0) GO TO 91
      DO 83 JQ=1,LYM
      S5=JQ*Y2
      U1=S2*(COS(S5)+U*SIN(S5))
      DO 84 JP=1,LX
      J1=J1+1
      P(J1)=U1
   84 CONTINUE
   83 CONTINUE
   91 DO 85 JQ=1,LY
      S5=(JQ-.5)*Y2
      U1=S1*(COS(S5)+U*SIN(S5))
      DO 86 JP=1,LXM
      J1=J1+1
      P(J1)=U1
   86 CONTINUE
   85 CONTINUE
      RETURN
      END
```

IV. DESCRIPTION OF THE SUBROUTINES DECOMP AND SOLVE

The subroutines DECOMP(N, IPS, UL) and SOLVE(N,IPS,UL,B,X) use the method of Gaussian elimination and LU decomposition described in [5, Section 9] to solve a linear system of equations with complex coefficients. DECOMP and SOLVE, based on the FORTRAN programs on pages 68 and 69 of [5], require roughly $\frac{n^3}{3}$ multiplicative operations to solve a system of n linear equations whereas the subroutine LINEQ on pages 28 and 29 of [2] requires roughly n^3 multiplicative operations to solve the same system.

The input into DECOMP is N and the matrix [A] of coefficients of the set

$$[A]\vec{x} = \vec{b} \tag{69}$$

of N linear equations stored by columns in UL. $N \geq 2$. The output from DECOMP is IPS and UL. DECOMP does not change N. SOLVE uses N, IPS, UL, and the elements of $\vec{b}$ stored in B to calculate and store in X the elements of the solution vector $\vec{x}$. SOLVE does not change any of the input variables N, IPS, UL and B. Minimum allocations are given by

```
COMPLEX UL(N*N)
DIMENSION SCL(N), IPS(N)
```

in DECOMP and by

```
COMPLEX UL(N*N), B(N), X(N)
DIMENSION IPS(N)
```

in SOLVE.

Assuming that the reader is familiar with [5, Section 9], we will attempt to explain interchanging rows and scaling by rows [5, Sections 10 and 11]. Interchanging rows is necessary to avoid pivots which are close to zero. The divisors a_{11}, $a_{22}^{(2)}$ and $a_{33}^{(3)}$ of [5, Section 9] are called pivots. Scaling the matrix by rows facilitates the search for pivots by insuring that the number with the largest magnitude is most likely the best pivot.

It will be shown that interchanging the ith and jth rows of the array UL in storage at any stage of the computation is equivalent to

[5] G. E. Forsythe and C. B. Moler, "Computer Solution of Linear Albegraic Systems," Prentice-Hall, Inc., Englewood Cliffs, New Jersey, 1967.

interchanging the ith and jth elements of $\vec{b}$. The above statement is certainly true if the row interchange occurs at the very beginning when [A] resides in UL. After zeros have been introduced in the below the main diagonal positions of the first m columns of A,

$$UL = \begin{bmatrix} A^{11} & A^{12} \\ \\ A^{21} & A^{22} \end{bmatrix} \tag{70}$$

where A^{11} is an m by m submatrix. The elements of A^{11} on and above the main diagonal and all the elements of A^{12} and A^{22} are elements of $[M_m M_{m-1} \ldots M_1 A]$ where M_j is defined in [5, Section 9]. The elements of A^{11} strictly below the main diagonal and all the elements of A^{21} are elements of $[M_m M_{m-1} \ldots M_1]^{-1}$. Hence,

$$\begin{bmatrix} B^{11} & 0 \\ A^{21} & U \end{bmatrix} \begin{bmatrix} C^{11} & A^{12} \\ 0 & A^{22} \end{bmatrix} \vec{x} = \vec{b}' \tag{71}$$

where B^{11} is a lower triangular matrix whose main diagonal elements are equal to unity and whose elements below the main diagonal are equal to those of A^{11}, C^{11} is an upper triangular matrix whose elements on and above the main diagonal are equal to those of A^{11}, U is an identity matrix, and $\vec{b}'$ is $\vec{b}$ with its elements permuted in accordance with any previous row interchanges which may have occurred. From (71),

$$\begin{bmatrix} B^{11}\,C^{11} & B^{11}\,A^{12} \\ \\ A^{21}\,C^{11} & A^{21}A^{12} + A^{22} \end{bmatrix} \vec{x} = \vec{b}' \tag{72}$$

At the stage at which UL is given by (70), the row interchange is limited to the last m+1 rows of UL and hence only affects A^{21} and A^{22}. From (72), an interchange of two rows of A^{21} and A^{22} is equivalent to interchanging the corresponding two elements of $\vec{b}'$.

In DECOMP, the row interchanges are not done physically, but mentally by means of the variable IPS. The Ith row of the row interchanged array is the IPS(I)th row stored in UL.

Scaling by rows consists of multiplying all the elements of the jth row of A, j=1,2,...N, by the reciprocal, called SCL(j) in DECOMP, of the magnitude of the largest element in the jth row. In DECOMP, the rows of A are not scaled physically. The effect of physical scaling would, as deduced from the algorithm in [5, Section 9], be to multiply any jth row element involved in a search for a pivot by SCL(j). DECOMP obtains the effect of scaling by incorporating SCL into the searches for pivots.

A verbal flow chart of DECOMP(N,IPS,UL) is as follows. DO loop 5 initializes IPS and obtains SCL. In DO loop 2, the operation consisting of the sum of the absolute values of the real and imaginary parts ought to be more efficient than the usual magnitude involving the square root of the sums of the squares of the real and imaginary parts.

DO loop 17 performs the premultiplication by M_K where M_K is defined in [5, Section 9]. DO loop 11 decides that the (IPS(IPV),K)th element of UL will be the pivot. If we were using the method of physical row interchanges we would, at this point, interchange the Kth and IPVth rows physically. Statements 14 and the two statements following it carry out the corresponding mental row interchange by interchanging IPS(IPV) and IPS(K). Nested DO loops 16 subtract m_{IK} times the IPS(K)th row of UL from the last K+1 columns of the IPS(I)th row of UL. See [5, Section 9] for the definition of m_{IK}. Note that m_{IK} is such that the previous row operation extended to the Kth column would annihilate the (IPS(I),K)th element of UL. Statement 18 stores m_{IK} in the (IPS(I),K)th position of UL.

The subroutine SOLVE(N,IPS,UL,B,X) obtains the solution $\vec{x}$ to

$$[L][U]\vec{x} = \vec{b}' \tag{73}$$

where [L] is a lower triangular matrix whose diagonal elements are all unity and [U] is an upper triangular matrix. Here, U_{ij}, $j \geq i$, is stored in the (IPS(i), j)th position of the input array UL. Also, $L_{ii} = 1$ and L_{ij}, $i > j$ is stored in the (IPS(i),j)th position of UL. The ith element of b' is stored in B(IPS(i)). As in [5, Section 9], we let

$$[U]\vec{x} = \vec{y} \tag{74}$$

such that (73) becomes

$$[L]\vec{y} = \vec{b}' \tag{75}$$

The solution to (75) is given by

$$y_1 = b_1' \tag{76}$$

$$y_i = b_i' - \sum_{j=1}^{i-1} L_{ij} y_j \,, \qquad i = 2,3,\ldots N$$

The solution to (74) is given by

$$x_N = \frac{y_N}{U_{NN}}$$

$$x_i = \frac{y_i - \sum_{j=i+1}^{N} U_{ij} x_j}{U_{ii}} \,, \quad i=N-1,\ N-2,\ldots 1 \tag{77}$$

A verbal flow chart of the subroutine SOLVE(N,IPS,UL,B,X) is as follows. DO loop 2 stores y_I of (76) in X(I). The index J of inner DO loop 1 is the summation index j appearing in (76). DO loop 4 stores x_i of (77) in X(i) for i = N+1 - IBACK. The index J of inner DO loop 3 is the summation index j appearing in (77).

```
C     LISTINGS OF THE SUBROUTINES DECOMP AND SOLVE
C
      SUBROUTINE DECOMP(N,IPS,UL)
      COMPLEX UL(2500),PIVOT,EM
      DIMENSION SCL(50),IPS(50)
      DO 5 I=1,N
      IPS(I)=I
      RN=0.
      J1=I
      DO 2 J=1,N
      ULM=ABS(REAL(UL(J1)))+ABS(AIMAG(UL(J1)))
      J1=J1+N
      IF(RN-ULM) 1,2,2
    1 RN=ULM
    2 CONTINUE
      SCL(I)=1./RN
    5 CONTINUE
      NM1=N-1
      K2=0
      DO 17 K=1,NM1
      BIG=0.
      DO 11 I=K,N
      IP=IPS(I)
      IPK=IP+K2
      SIZE=(ABS(REAL(UL(IPK)))+ABS(AIMAG(UL(IPK))))*SCL(IP)
      IF(SIZE-BIG) 11,11,10
   10 BIG=SIZE
      IPV=I
   11 CONTINUE
      IF(IPV-K) 14,15,14
   14 J=IPS(K)
      IPS(K)=IPS(IPV)
      IPS(IPV)=J
   15 KPP=IPS(K)+K2
      PIVOT=UL(KPP)
      KP1=K+1
      DO 16 I=KP1,N
      KP=KPP
      IP=IPS(I)+K2
      EM=-UL(IP)/PIVOT
   18 UL(IP)=-EM
      DO 16 J=KP1,N
      IP=IP+N
      KP=KP+N
      UL(IP)=UL(IP)+EM*UL(KP)
   16 CONTINUE
      K2=K2+N
   17 CONTINUE
      RETURN
      END
      SUBROUTINE SOLVE(N,IPS,UL,B,X)
      COMPLEX UL(2500),B(50),X(50),SUM
      DIMENSION IPS(50)
      NP1=N+1
      IP=IPS(1)
      X(1)=B(IP)
      DO 2 I=2,N
      IP=IPS(I)
      IPB=IP
      IM1=I-1
```

```
      SUM=0.
      DO 1 J=1,IM1
      SUM=SUM+UL(IP)*X(J)
    1 IP=IP+N
    2 X(I)=B(IPB)-SUM
      K2=N*(N-1)
      IP=IPS(N)+K2
      X(N)=X(N)/UL(IP)
      DO 4 IBACK=2,N
      I=NP1-IBACK
      K2=K2-N
      IPI=IPS(I)+K2
      IP1=I+1
      SUM=0.
      IP=IPI
      DO 3 J=IP1,N
      IP=IP+N
    3 SUM=SUM+UL(IP)*X(J)
    4 X(I)=(X(I)-SUM)/UL(IPI)
      RETURN
      END
```

REFERENCES

[1] R. F. Harrington and J. R. Mautz, "A Generalized Network Formulation for Aperture Problems," Scientific Report No. 8 on Contract F19628-73-C-0047 with A.F. Cambridge Research Laboratories, Report AFCRL-TR-75-0589, November 1975.

[2] J. R. Mautz and R. F. Harrington, "Electromagnetic Transmission Through a Rectangular Aperture in a Perfectly Conducting Plane," Scientific Report No. 10 on Contract F19628-73-C-0047, with A.F. Cambridge Research Laboratories, Report AFCRL-TR-76-0056, February 1976.

[3] R. F. Harrington, "Time-Harmonic Electromagnetic Fields," McGraw-Hill Book Company, New York, 1961, Equations (8-34), (3-86), and (3-89) and Section 4-3.

[4] M. Cohen, T. Crowley, K. Levis, "The Aperture Admittance of a Rectangular Waveguide Radiating into Half-Space," Antenna Lab. Rept. ac 21114 S.R. No. 22, Ohio State University, 1953.

[5] G. E. Forsythe and C. B. Moler, "Computer Solution of Linear Algebraic Systems," Prentice-Hall, Inc., Englewood Cliffs, New Jersey, 1967.

MISSION
of
Rome Air Development Center

RADC plans and conducts research, exploratory and advanced development programs in command, control, and communications (C^3) activities, and in the C^3 areas of information sciences and intelligence. The principal technical mission areas are communications, electromagnetic guidance and control, surveillance of ground and aerospace objects, intelligence data collection and handling, information system technology, ionospheric propagation, solid state sciences, microwave physics and electronic reliability, maintainability and compatibility.

AMERICAN REVOLUTION BICENTENNIAL 1776-1976

Printed by
United States Air Force
Hanscom AFB, Mass. 01731